Metastability in the stochastic nearest-neighbor Kuramoto model of coupled phase oscillators

Nils Berglund, Georgi S. Medvedev, and Gideon Simpson

December 19, 2024

Abstract

The Kuramoto model (KM) of n coupled phase-oscillators is analyzed in this work. The KM on a Cayley graph possesses a family of steady state solutions called twisted states. Topologically distinct twisted states are distinguished by the winding number $q \in \mathbb{Z}$. It is known that for the KM on the nearest-neighbor graph, a q-twisted state is stable if $|q| < n/4$. In the presence of small noise, the KM exhibits metastable transitions between q–twisted states. Specifically, a typical trajectory remains in the basin of attraction of a given q-twisted state for an exponentially long time, but eventually transitions to the vicinity of another such state. In the course of this transition, it passes in close proximity of a saddle of Morse index 1, called a relevant saddle. In this work, we provide an exhaustive analysis of metastable transitions in the stochastic KM with nearest-neighbor coupling.

We start by analyzing the equilibria and their stability. First, we identify all equilibria in this model. Using the discrete Fourier transform and eigenvalue estimates for rank–1 perturbations of symmetric matrices, we classify the equilibria by their Morse indices. In particular, we identify all stable equilibria and all relevant saddles involved in the metastable transitions. Further, we use Freidlin–Wentzell theory and the potential-theoretic approach to metastability to establish the metastable hierarchy and sharp estimates of Eyring–Kramers type for the transition times. The former determines the precise order, in which the metastable transitions occur, while the latter characterizes the times between successive transitions. The theoretical estimates are complemented by numerical simulations and a careful numerical verification of the transition times. Finally, we discuss the implications of this work for the KM with other coupling types including nonlocal coupling and the continuum limit as n tends to infinity.

2020 *Mathematical Subject Classification.* 60H10, 34F05, 60K35, 92B20.
Keywords and phrases. Phase oscillators, Kuramoto model, noise, metastability, synchronization.

1 Introduction

The Kuramoto model (KM) of coupled phase oscillators provides an important framework for studying collective behavior in diverse natural and man-made networks ranging from interacting particle models in statistical physics [24], to neuronal networks and swarms of fireflies [37] in biology, to power grids in engineering [15]. It has been extremely useful in revealing new facets of well-known phenomena in coupled networks such as synchronization [12,24,36] and multistability [38], as well as in identifying new effects such as chimera states [1, 23]. In this work, we use the KM to study metastability as a mechanism of pattern formation in dynamical networks forced by small noise.

We begin by introducing the KM with identical intrinsic frequencies (cf. [38]):

$$\dot{u}_i = K \sum_{j \in S} \sin\left(2\pi(u_{i+j} - u_i)\right) , \tag{1.1}$$

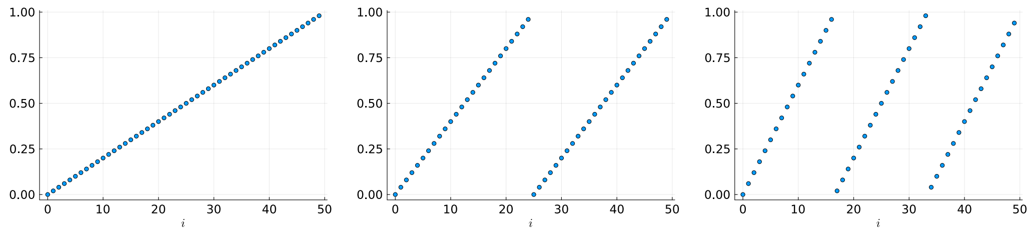

(a) $q = 1$ (b) $q = 2$ (c) $q = 3$

Figure 1: Examples of q-twisted state equilibria with $n = 50$. The plots represent $u_i^{(q,0)}$ as a function of i.

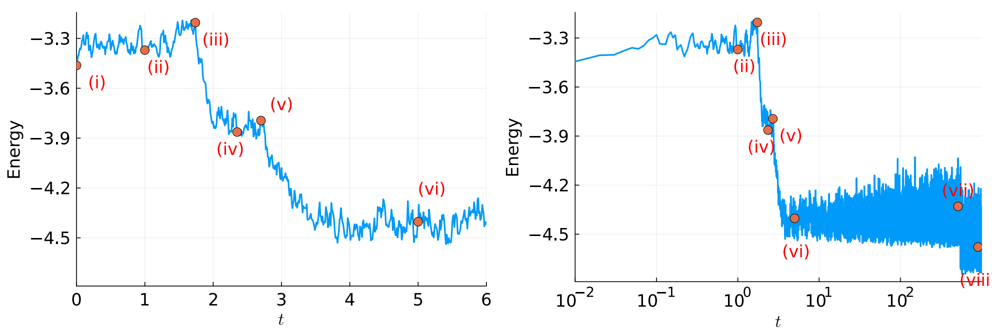

(a) (b)

Figure 2: Energy of the Kuramoto system with $n = 20$ as a function of time. Labeled points correspond to approximate local minima and transition states that are shown in Figure 3. Figure (b) is a continuation of (a) on a longer time scale.

where $K > 0$ is the coupling strength, $i \in \Lambda = \mathbb{Z}/n\mathbb{Z}$, and S is a finite symmetric set subset of $\Lambda\backslash\{0\}$, i.e., $S \subset \Lambda\backslash\{0\}$ and $-s \in S$ whenever $s \in S$. In addition, let $r = |S|/2$ denote the range of coupling. For the most part, we will deal with the nearest neighbor coupling $S = \{-1, 1\}$ and $r = 1$.

The KM (1.1) has a family of steady state solutions $u^{(q,\varphi)}$ of the form

$$u_i^{(q,\varphi)} = \frac{qi}{n} + \varphi \,, \qquad i \in \Lambda$$

for any integer q such that $-\frac{n}{2} < q \leqslant \frac{n}{2}$ and $\varphi \in [0, 1)$. See Figure 1 for some examples. These are called *q-twisted states* (cf. [38]). The stability of a q-twisted state can be determined from an explicit condition on q, r, and n (cf. [29, Theorem 3.4]). In particular, it can be shown that for $r \ll n$ there are multiple stable q-twisted states.

In this paper, we study the behavior of solutions of (1.1) under weak stochastic forcing. To this end, we rewrite it as a gradient system and add a stochastic forcing term on the right hand side, yielding the stochastic differential equation (SDE)

$$\mathrm{d}u_t = -\nabla U(u_t)\,\mathrm{d}t + \sqrt{2\varepsilon}\,\mathrm{d}W_t \,. \tag{1.2}$$

Here U is the potential (or energy function) on $(\mathbb{S}^1)^\Lambda$ given by

$$U(u) = -\frac{K}{4\pi}\sum_{i\in\Lambda}\sum_{j\in S}\cos\bigl(2\pi(u_{i+j} - u_i)\bigr) \,, \tag{1.3}$$

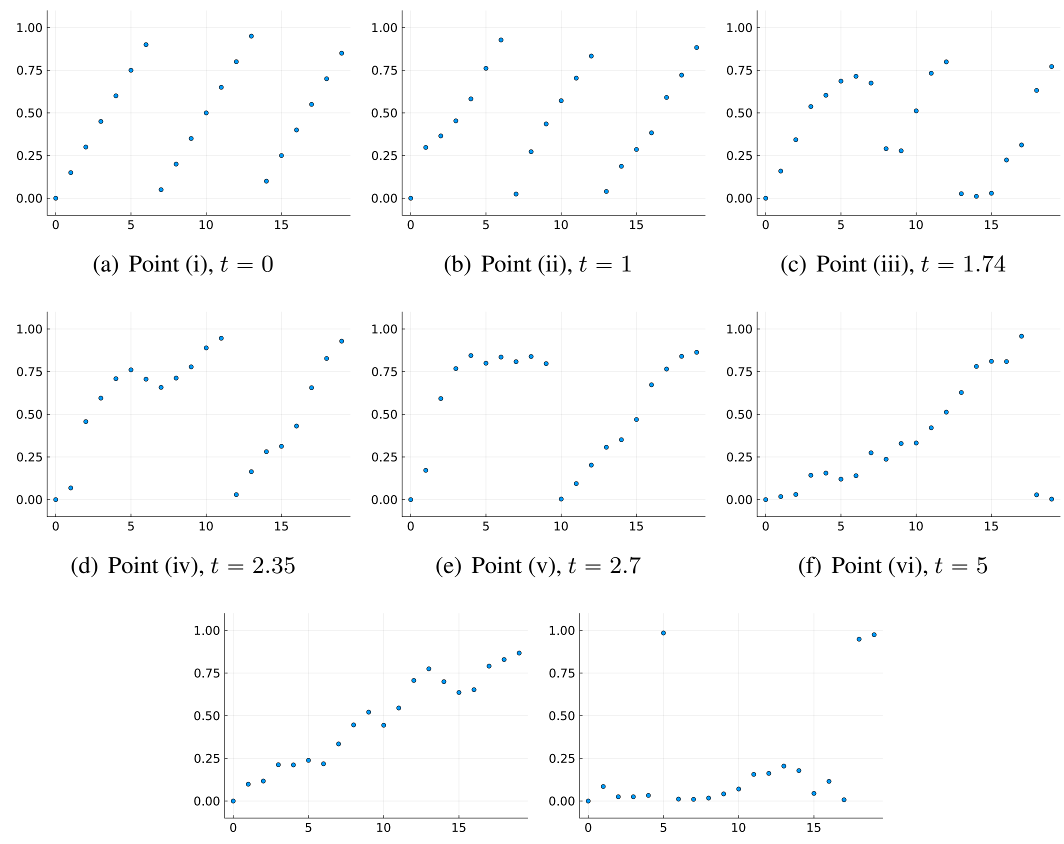

(a) Point (i), $t = 0$
(b) Point (ii), $t = 1$
(c) Point (iii), $t = 1.74$
(d) Point (iv), $t = 2.35$
(e) Point (v), $t = 2.7$
(f) Point (vi), $t = 5$
(g) Point (vii), $t = 510.65$
(h) Point (viii), $t = 900$

Figure 3: The characteristic states visited by the trajectory in the course of a transition from the 3-twisted state to the 0-twisted state shown in Figure 2.

W_t is an n-dimensional standard Wiener process, and $\varepsilon > 0$ is a small parameter controlling the standard deviation of the noise.

In the presence of noise, the KM exhibits metastable transitions between neighboring twisted states. For illustration, we discuss the example shown in Figures 2 and 3. The system initialized at a 3-twisted state undergoes a series of metastable transitions that take it through the basins of attraction of 2- and 1-twisted states before reaching the basin of attraction of a 0-twisted state. Figure 3 shows a few representative snapshots, illustrating both the states that are close to the attractors of the KM and the states close to the boundaries between the basins of attraction of the different twisted states. The main objective of this work is to determine which of these transitions are the most likely, determine the most likely order of these transitions, and to quantify the random time intervals between successive transitions.

The analysis in this paper relies on the Freidlin–Wentzell theory of large deviations [19] and the potential-theoretic approach to metastability [11], which allows for sharp asymptotics of the transition times. The description of metastability based on the Freidlin–Wentzell theory was formulated in [18] (see also [19, Chapter 6] and [32]). For the exposition of the potential-theoretic approach and for many different applications of metastability, we refer to [10]. Large deviations and metastability as the mechanisms driving dynamics of coupled networks have been studied, for instance, in [6, 7, 14, 20, 21, 25, 28]. In this work, through the careful analysis of the attractors and relevant saddles for the model at hand, we are able to establish the precise hierarchy of metastable

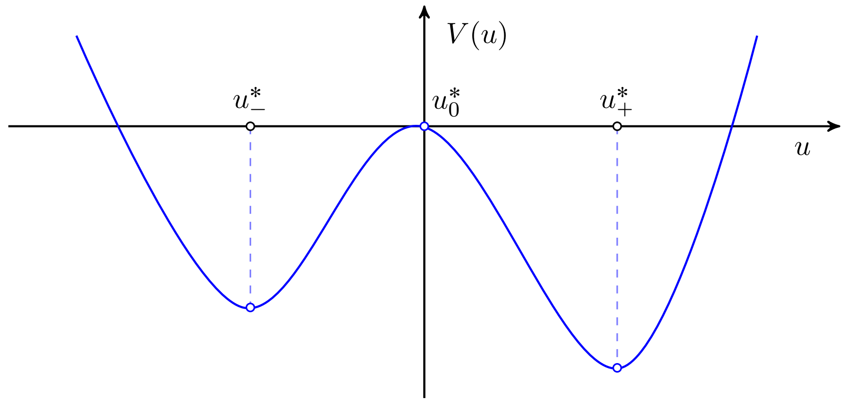

Figure 4: A one-dimensional double-well potential.

transitions and to obtain sharp estimates of the transition times. The results of this work show that coupled systems of simple phase oscillators with identical intrinsic velocities exhibit interesting metastable dynamics due to complex energy landscape.

The remainder of this article is organized as follows. In Section 2, we recall some known properties of gradient systems perturbed by weak Gaussian noise, based on the Freidlin–Wentzell theory of large deviations [19], and the Eyring–Kramers law [2, 11]. This theory has to be adapted to the model at hand, owing to symmetries of the potential U. We give a description of this procedure in Section 3. In Section 4, we provide a detailed analysis of the equilibrium states of the system. In particular, we obtain a complete list of stable states and of all relevant saddles. Section 5 contains the main analytical result of this work, Theorem 5.4, which gives sharp Eyring–Kramers asymptotics for the expected transition time from less stable to more stable q-twisted states. This section also contains a discussion of the computation of some more general transition times. Section 6 illustrates the results with numerical simulations, and Section 7 provides concluding remarks and an outlook.

2 Stochastically perturbed systems

Consider a finite-dimensional SDE of the form

$$\mathrm{d}u_t = -\nabla V(u_t)\,\mathrm{d}t + \sqrt{2\varepsilon}\,\mathrm{d}W_t \tag{2.1}$$

on $\mathbb{R}^n$, where W_t is an n-dimensional standard Wiener process.

Assume first that V is a double-well potential, having local minima at u^*_- and u^*_+ (Figure 4), and that the Hessian matrix of V at u^*_- has eigenvalues

$$0 < \lambda_1 \leqslant \lambda_2 \leqslant \cdots \leqslant \lambda_n\ .$$

Suppose $G \ni u^*_-$ is an open set contained in the basin of attraction of u^*_-. Consider a trajectory of (2.1) starting at $u_0 \in G$. After staying in G for a time of order $\mathrm{e}^{C/\varepsilon}$, for some $C > 0$, it eventually leaves the basin of attraction of u^*_- with probability 1 (cf. [19]). On its way, it passes with high probability through the vicinity of a saddle u^*_0, on the boundary of the basins of attraction of the two local minima of the double-well potential. Assume that this saddle is unique and the Hessian matrix of V at the saddle has eigenvalues

$$\mu_1 < 0 < \mu_2 \leqslant \mu_3 \leqslant \cdots \leqslant \mu_n\ .$$

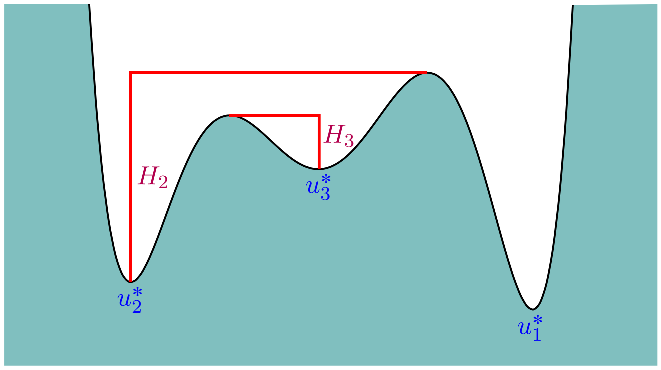

Figure 5: Example of metastable hierarchy. The relevant relative communication heights are $H_3 = \overline{V}(u_3^*, \{u_1^*, u_2^*\}) - V(u_3^*)$ and $H_2 = \overline{V}(u_2^*, \{u_1^*\}) - V(u_2^*)$.

The Eyring–Kramers law states that if the system starts near u_-^*, and ε is small, then the expected time needed to reach a neighborhood of u_+^* is given by

$$\begin{aligned} \mathbb{E}^{u_-^*}\{\tau_+\} &= \frac{2\pi}{|\mu_1|}\sqrt{\frac{\bigl|\det\bigl[\frac{\partial^2 V}{\partial^2 u}(u_0^*)\bigr]\bigr|}{\det\bigl[\frac{\partial^2 V}{\partial^2 u}(u_-^*)\bigr]}}\,\mathrm{e}^{[V(u_0^*)-V(u_-^*)]/\varepsilon}\bigl[1+R(\varepsilon)\bigr] \\ &= 2\pi\sqrt{\frac{\mu_2\dots\mu_n}{|\mu_1|\lambda_1\dots\lambda_n}}\,\mathrm{e}^{[V(u_0^*)-V(u_-^*)]/\varepsilon}\bigl[1+R(\varepsilon)\bigr]\;, \end{aligned} \tag{2.2}$$

where $\frac{\partial^2 V}{\partial^2 u}$ stands for the Hessian matrix of V, and $R(\varepsilon)$ is a remainder going to 0 as $\varepsilon \to 0$ (one usually has information on how fast this happens).

This result has been extended to potentials with more than two wells, provided one has a so-called *metastable hierarchy*. Given two points $u, v \in \mathbb{R}^n$, we call *path connecting u to v* a continuous map $\gamma : [0,1] \to \mathbb{R}^n$ such that $\gamma(0) = u$ and $\gamma(1) = v$. In that case, we write $\gamma : u \to v$. The *communication height from u to v* is defined as

$$\overline{V}(u,v) = \inf_{\gamma: u\to v}\sup_{t\in[0,1]} V(\gamma(t))\;.$$

This can be generalized to the communication height between two sets $A, B \subset \mathbb{R}^n$ by

$$\overline{V}(A,B) = \inf_{u\in A, v\in B}\overline{V}(u,v)\;.$$

A *minimal path from A to B* is any path $\gamma : u \to v$, with $u \in A$ and $v \in B$, such that

$$\sup_{t\in[0,1]} V(\gamma(t)) = \overline{V}(A,B)\;.$$

If there is a finite set of points $w_1, \dots, w_p \in \mathbb{R}^n$ such that $V(w_1) = \dots = V(w_p) = \overline{V}(A,B)$, and any minimal path γ from A to B contains at least one of these points, then the w_i are called *relevant saddles* between A and B. In fact, in the generic case the relevant saddle is unique, provided A and B are contained in the basins of attraction of two different local minima of the potential (see [8, Section 2.1] for more details). A related approach for determining the metastable hierarchy can be found in [19, Chapter 6, § 6].

With this terminology in place, we can now define the notion of metastable hierarchy. Assume that the potential V has a finite set $\{u_1^*, \dots u_{N_0}^*\}$ of local minima. For any $k \in \{1, \dots, N_0\}$, we define the metastable set $\mathcal{M}_k = \{u_1^*, \dots, u_k^*\}$. For each $k \in \{2, \dots, N_0\}$, we define the *relative communication height*

$$H_k = \overline{V}(u_k^*, \mathcal{M}_{k-1}) - V(u_k^*) .$$

The quantity H_k yields the barrier in the potential landscape that one needs to overcome to reach $\mathcal{M}_{k-1}$ from u_k^*. We say that the u_i^* are in metastable order, and write $u_1^* \prec u_2^* \prec \dots u_{N_0}^*$, if there exists $\theta > 0$ such that

$$H_k \leqslant \min_{i \leqslant k} \big[\overline{V}(u_i^*, \mathcal{M}_{k-1}) - V(u_i^*)\big] - \theta$$

holds for $k \in \{2, \dots, N_0\}$. Intuitively, this means that the minima are arranged in the order of difficulty for escape. The easiest transition is from $u_{N_0}^*$ to $\mathcal{M}_{N_0-1}$, and the hardest transition is from u_2^* to $\mathcal{M}_1 = \{u_1^*\}$. Figure 5 gives an example with $N_0 = 3$.

Assume that all local minima are non-degenerate, and that for each $k \in \{2, \dots, N_0\}$, there is a unique relevant saddle $\hat{u}_k^*$ between u_k^* and $\mathcal{M}_{k-1}$, which is also non-degenerate. Then Theorem 3.2 in [11] shows that the first hitting time τ_{k-1} of $\mathcal{M}_{k-1}$, starting from u_k^*, satisfies

$$\mathbb{E}^{u_k^*}\big\{\tau_{k-1}\big\} = \frac{2\pi}{|\mu_1(k)|} \sqrt{\frac{\big|\det\big[\frac{\partial^2 V}{\partial^2 u}(\hat{u}_k^*)\big]\big|}{\det\big[\frac{\partial^2 V}{\partial^2 u}(u_k^*)\big]}} \, \mathrm{e}^{H_k/\varepsilon}\big[1 + R(\varepsilon)\big] ,$$

where $\mu_1(k)$ is the unique negative eigenvalue of the Hessian at $\hat{u}_k^*$. Note that the only difference with (2.2) lies in the points where the Hessians are evaluated.

Note that [11, Theorem 3.2] does not make any statement on other metastable transitions than the ones from u_k^* to $\mathcal{M}_{k-1}$. However, results in [3, 34, 35] show that the system can be approximated, in a suitable sense, by a continuous-time Markov chain on the set of local minima. This allows estimating other expected transition times, in a way we illustrate in Section 5.3.

3 The potential landscape

In this section, we provide an analysis of symmetries of the potential landscape of the Kuramoto model (1.1). In particular, we construct a fundamental domain that accounts for the angular nature of the variables u_i, and show how the degeneracy of the potential under global phase shifts can be dealt with by a simple change of variables.

We will focus on the nearest-neighbor coupling case $S = \{-1, 1\}$. Then the Kuramoto potential (1.3) can be written as

$$U(u) = -\frac{K}{2\pi} \sum_{i \in \Lambda} \cos(2\pi(u_{i+1} - u_i)) , \tag{3.1}$$

which can be viewed as a function from $\mathbb{R}^\Lambda$ to $\mathbb{R}$ (or, equivalently, from $\mathbb{R}^n$ to $\mathbb{R}$). This potential has a large symmetry group, which has important implications on the analysis.

3.1 Symmetries

A *symmetry* is a map $g : \mathbb{R}^\Lambda \to \mathbb{R}^\Lambda$ such that

$$U(g(u)) = U(u) \qquad \forall u \in \mathbb{R}^\Lambda .$$

The potential (3.1) has the following symmetries:

1. **Integer translations:**

$$T_k(u_0, \ldots, u_{n-1}) = (u_0 + k_0, \ldots, u_{n-1} + k_{n-1}) , \qquad k \in \mathbb{Z}^\Lambda \simeq \mathbb{Z}^n .$$

This is due to the 2π-periodicity of $\sin$.

2. **Global phase shift:**

$$S_\varphi(u_0, \ldots, u_{n-1}) = (u_0 + \varphi, \ldots, u_{n-1} + \varphi) , \qquad \varphi \in \mathbb{R} .$$

This is due to the translation invariance of the KM.

3. **Cyclic permutation of components:**

$$C_p(u_0, \ldots, u_{n-1}) = (u_p, \ldots, u_{n-1+p}) , \qquad p \in \Lambda . \tag{3.2}$$

This is due to nearest neighbors having the same interaction.

4. **Inversion:**

$$I(u_0, \ldots, u_{n-1}) = (-u_0, \ldots, -u_{n-1}) .$$

This follows from the fact that the interaction with the left and right neighbor are the same.

It will be convenient to take as phase space a fundamental domain with respect to the first two types of symmetries. This means that we consider two points $u, v \in \mathbb{R}^\Lambda$ to be equivalent if, and only if, there exist $k \in \mathbb{Z}^\Lambda$ and $\varphi \in \mathbb{R}$ such that $v = T_k S_\varphi u$. A *fundamental domain* (or *unit cell*) is then a set $\mathcal{D}$ of representatives of the equivalence classes defined by this equivalence relation.

If we only considered integer translations, a natural choice of fundamental domain would be the torus $\mathbb{T}^\Lambda = \mathbb{R}^\Lambda / \mathbb{Z}^\Lambda$ (or, equivalently, $\mathbb{T}^n = \mathbb{R}^n / \mathbb{Z}^n$). However, since we also consider global phase shifts, we proceed differently. We first define the hyperplane

$$\Sigma = \{u \in \mathbb{R}^\Lambda \colon u_0 + \cdots + u_{n-1} = 0\} .$$

This hyperplane corresponds to modding out global phase shifts, the representative of a point $u \in \mathbb{R}^\Lambda$ being simply its orthogonal projection on Σ.

We now want to account for integer translations as well. If $k = (k_0, \ldots, k_{n-1})^\top \in \mathbb{Z}^\Lambda$ is a point with integer coordinates, its orthogonal projection on Σ has coordinates

$$\begin{aligned} k - \frac{1}{n}\langle k, \mathbf{1} \rangle \mathbf{1} &= \frac{1}{n}\big((n-1)k_1 - k_2 - \cdots - k_n, -k_1 + (n-1)k_2 - k_3 - \cdots - k_n, \ldots)\big)^\top \\ &= \sum_{i=0}^{n-1} k_i v_i , \end{aligned} \tag{3.3}$$

where

$$\mathbf{1} = \big(1, \ldots, 1\big)^\top \in \mathbb{R}^\Lambda , \tag{3.4}$$

and

$$\begin{aligned} v_0 &= \big(1 - \tfrac{1}{n}, -\tfrac{1}{n}, \ldots, -\tfrac{1}{n}\big)^\top , \\ v_1 &= \big(-\tfrac{1}{n}, 1 - \tfrac{1}{n}, \ldots, -\tfrac{1}{n}\big)^\top , \\ &\ldots \\ v_{n-1} &= \big(-\tfrac{1}{n}, \ldots, -\tfrac{1}{n}, 1 - \tfrac{1}{n}\big)^\top . \end{aligned}$$

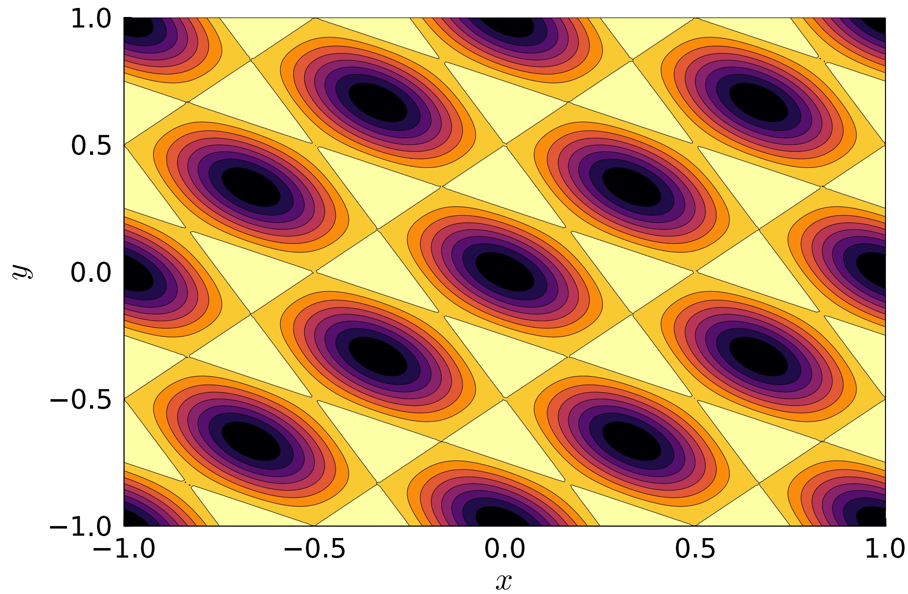

Figure 6: Contour plot of the potential (3.5), obtained by restricting the Kuramoto potential (1.3) to the hyperplane Σ, for $n = 3$. The hexagons are basins of attraction of the 0-twisted state $u^{(0)}$ and its translates, while the triangles contain local maxima of the potential.

The set of vectors $(v_0, \dots, v_{n-2})$ forms a (non-orthonormal) basis of Σ. The projections (3.3) form a lattice given by integer linear combinations of these vectors.

This motivates the choice of fundamental domain

$$\mathcal{D} = \left\{ y_0 v_0 + \dots + y_{n-2} v_{n-2} \colon -\tfrac{1}{2} \leqslant y_i < \tfrac{1}{2}, i = 0, \dots, n-2 \right\} .$$

Example 3.1. Consider the case $n = 3$. Using the fact that $u_2 = -u_1 - u_0$ if $u \in \Sigma$, we obtain

$$U(u) = -\frac{K}{2\pi} \Big[\cos\big(2\pi(u_1 - u_0)\big) + \cos\big(2\pi(u_0 + 2u_1)\big) + \cos\big(2\pi(2u_0 + u_1)\big) \Big] . \tag{3.5}$$

Figure 6 shows a contour plot of this function. The fundamental domain $\mathcal{D}$ is a parallelogram with vertices $\pm(\frac{1}{6}, \frac{1}{6})^\top$ and $\pm(\frac{1}{2}, -\frac{1}{2})^\top$. In y-coordinates, the expression for the potential becomes

$$U(y_0 v_0 + y_1 v_1) = -\frac{K}{2\pi} \Big[\cos\big(2\pi(y_1 - y_0)\big) + \cos\big(2\pi y_1\big) + \cos\big(2\pi y_0\big) \Big] . \tag{3.6}$$

The following result gives an explicit expression for the coordinate transformation between the u_i and the y_j.

Lemma 3.2. *If $u = \sum_{i=0}^{n-2} y_i v_i$, then for any $i \in \{0, \dots, n-2\}$ one has*

$$y_i \equiv u_i + \sum_{j=0}^{n-2} u_j , \qquad u_i \equiv y_i - \frac{1}{n} \sum_{j=0}^{n-2} y_j , \tag{3.7}$$

where $\equiv$ stands for equality modulo 1.

Proof. The transformation from y to u can be written $u = My$, where $M = \mathbb{1}_{n-1} - \frac{1}{n} \mathbf{1}_{n-1} \mathbf{1}_{n-1}^\top$. Here $\mathbf{1}_{n-1}$ denotes the vector of dimension $n-1$ having all components equal to 1, and $\mathbb{1}_{n-1}$ is the identity matrix of dimension $n-1$. Using the fact that $\mathbf{1}_{n-1}^\top \mathbf{1}_{n-1} = n-1$, one easily checks that $M^{-1} = \mathbb{1}_{n-1} + \mathbf{1}_{n-1} \mathbf{1}_{n-1}^\top$. □

3.2 Changing coordinates

The results on metastability outlined in Section 2 do not apply directly to the stochastically forced KM (1.2), because the Hessian matrix at any equilibrium point has a zero eigenvalue, as a consequence of the translation invariance of the potential. This can be remedied by a change of variables compatible with our choice of fundamental domain. A similar system of coordinates was used in the analysis of synchronization in [28, § 5.1].

Let

$$q_0 = \frac{1}{\sqrt{n}}\mathbf{1} ,$$

where $\mathbf{1}$ has been defined in (3.4), and choose $q_1, q_2, \dots, q_{n-1} \in \mathbb{R}^\Lambda$ such that $q_0, q_1, q_2, \dots, q_{n-1}$ form an orthonormal basis in $\mathbb{R}^\Lambda \simeq \mathbb{R}^n$. Let

$$Q = (q_1, q_2, \dots, q_{n-1}) \in \mathbb{R}^{n\times(n-1)} .$$

Then the change of variables

$$u_t = \bar{u}_t q_0 + Q v_t, \qquad \bar{u}_t \in \mathbb{R} , \quad v_t \in \mathbb{R}^{n-1}$$

yields the system

$$\begin{aligned} \mathrm{d}\bar{u}_t &= \sqrt{2\varepsilon}\,\mathrm{d}\widehat{W}^0_t , \\ \mathrm{d}v_t &= Q^\top \nabla U(Qv - \bar{u}q_0) + \sqrt{2\varepsilon}\,\mathrm{d}\widehat{W}_t , \end{aligned}$$

where $\widehat{W}^0_t$ and $\widehat{W}_t$ are independent standard Brownian motions, of respective dimensions 1 and $n-1$. Here we have used $\mathbf{1}^\top \nabla U = 0$, due to the translation invariance of U, the facts that $Q^\top Q = \mathbb{1}_{n-1}$, and $Q^T q_0 = 0$ (both because the change of variables is orthogonal), and the invariance of Brownian motion under rotations. Furthermore

$$Q^\top \nabla U(Qv - \bar{u}q_0) = Q^\top \nabla U(Qv) = \nabla_v V(v) ,$$

where $V(v) = U(Qv)$, and we have again used translation invariance of U. It follows that the dynamics can be described by the set of equations

$$\begin{aligned} \mathrm{d}\bar{u}_t &= \sqrt{2\varepsilon}\,\mathrm{d}\widehat{W}^0_t , \\ \mathrm{d}v_t &= \nabla_v V(v_t) + \sqrt{2\varepsilon}\,\mathrm{d}\widehat{W}_t . \end{aligned}$$

In this system, the evolutions of $\bar{u}_t$ and v_t are completely decoupled. The component $\bar{u}_t$ performs a simple Brownian motion, of variance $2\varepsilon t$, while v_t obeys an $(n-1)$-dimensional SDE in the hyperplane Σ, which will in general be non-degenerate. The dynamics of v_t can be mapped to an SDE on $\mathcal{D}$ with periodic boundary conditions.

Remark 3.3. *There is one difference between the equation on Σ and its projection on $\mathcal{D}$. While the latter admits an invariant probability measure, with density proportional to $\mathrm{e}^{-V(v)/\varepsilon}$, the former does not admit such a measure, because Σ is unbounded. This is because on large scales, the behavior of the process in Σ is closer to that of a random walk.*

In what follows, it will be more convenient to work in variables u instead of v, because this simplifies the computation of equilibrium points and Hessian matrices. The two points of view are, however, equivalent, if one disregards the zero eigenvalues of the Hessians in the direction $\mathbf{1}$.

4 The equilibria

In this section, we analyze the equilibria of (1.1). These are critical points of the potential U, meaning that they satisfy $\nabla U(u) = 0$. The Hessian matrix of U at a critical point has real eigenvalues, one of which is 0 due to the translation invariance of U. The *Morse index* of a critical point is the number of strictly negative eigenvalues of the Hessian.

We will be particularly interested in two types of equilibria, which are important for the description of the metastable transitions in the stochastically forced model (1.2). The first type consists in critical points of Morse index 0, which are local minima of U. Because of the vanishing eigenvalue, they are neutrally stable in the n-dimensional phase space, but asymptotically stable for the dynamics restricted to the hyperplane Σ. For that reason, we are going to call them *sinks*. The second type of important critical points are those having Morse index 1. We will call them 1-*saddles* for brevity. The important feature of the potential landscape in relation to understanding stochastic dynamics is how sinks are connected by minimal paths, in particular, which 1-saddles lie on these paths.

We restrict to the nearest-neighbor coupling case $S = \{-1, 1\}$, for which we can present a more complete picture.

4.1 Classification of equilibria

An equilibrium of (1.1) has to satisfy the equations

$$\sin\bigl(2\pi(u_{i+1} - u_i)\bigr) = \sin\bigl(2\pi(u_i - u_{i-1})\bigr) , \qquad i \in \Lambda . \tag{4.1}$$

Let us write

$$a_i = (u_{i+1} - u_i) \pmod 1 .$$

An equilibrium point is uniquely determined by the tuple $(a_0, \dots, a_{n-1})$. Note that due to the periodic boundary conditions, the sum $\omega = a_0 + \cdots + a_{n-1}$ is necessarily an integer, which must belong to $\{0, 1, \dots, n-1\}$. This integer can be interpreted as a *winding number*. For instance, the winding number of a q-twisted state is $q \pmod n$.

Relation (4.1) implies that for any $i \in \Lambda$, there are two options:

- either $a_{i+1} = a_i$,
- or $a_{i+1} = \frac{1}{2} - a_i \pmod 1$.

As a consequence, one of the following two cases holds:

1. All a_i have the same value a. Then the winding number is $\omega = na$. This corresponds to a q-twisted state, with $\omega = na = q \pmod n$. For future reference, we set $p = n$.
2. The a_i take two different values a and $\hat{a}$, related by $\hat{a} = \frac{1}{2} - a \pmod 1$. Notice that $\cos(2\pi a)$ and $\cos(2\pi\hat{a})$ have opposite sign. If $a \notin \{\frac{1}{4}, \frac{3}{4}\}$, we may assume that $\cos(2\pi a) > 0$, while $\cos(2\pi\hat{a}) < 0$. Then we set

   $$p = \#\{i : a_i = a\} = \#\{i : \cos(2\pi a_i) > 0\} .$$

   Since $a \neq \hat{a}$, we necessarily have $p \in \{1, \dots, n-1\}$, and it has to satisfy the condition

   $$pa + (n-p)\hat{a} = \omega . \tag{4.2}$$

   Note that $\hat{a} = \frac{1}{2} - a$ if $a < \frac{1}{2}$, and $\hat{a} = \frac{3}{2} - a$ otherwise.

In both cases, since we assume $S = \{-1, 1\}$, the potential can be written

$$U(u) = -\frac{K}{2\pi} \sum_{i\in\Lambda} \cos(2\pi(u_{i+1} - u_i)) = -\frac{K}{2\pi} \sum_{i\in\Lambda} \cos(2\pi a_i) \; . \tag{4.3}$$

Note that

$$\cos\bigl(2\pi a_i\bigr) = \sigma_i \cos(2\pi a) \qquad \text{where } \sigma_i = \begin{cases} 1 & \text{if } a_i = a \; , \\ -1 & \text{if } a_i = \hat{a} \; . \end{cases}$$

Therefore, we have

$$U(u) = -\frac{K}{2\pi} \cos(2\pi a) \sum_{i\in\Lambda} \sigma_i = -\frac{K}{2\pi}(2p - n)\cos(2\pi a) \; . \tag{4.4}$$

The stability of an equilibrium u is determined by the Hessian matrix of the potential at u, which can be written

$$\frac{\partial^2 U}{\partial u^2} = 2\pi K \cos\bigl(2\pi a\bigr) M(\sigma) \; , \tag{4.5}$$

where

$$M(\sigma) = \begin{pmatrix} \sigma_{n-1}+\sigma_0 & -\sigma_0 & 0 & \dots & \dots & 0 & -\sigma_{n-1} \\ -\sigma_0 & \sigma_0+\sigma_1 & -\sigma_1 & \ddots & & & 0 \\ 0 & -\sigma_1 & \sigma_1+\sigma_2 & \ddots & \ddots & & \vdots \\ \vdots & \ddots & \ddots & \ddots & \ddots & \ddots & \vdots \\ \vdots & & \ddots & \ddots & \ddots & -\sigma_{n-3} & 0 \\ 0 & & & \ddots & -\sigma_{n-3} & \sigma_{n-3}+\sigma_{n-2} & -\sigma_{n-2} \\ -\sigma_{n-1} & 0 & \dots & \dots & 0 & -\sigma_{n-2} & \sigma_{n-2}+\sigma_{n-1} \end{pmatrix} .$$

4.2 The sinks

For a q-twisted state $u^{(q)}$, all σ_i are equal to 1, and therefore $p = n$. The value (4.4) of the potential reduces to

$$U(u^{(q)}) = -\frac{K}{2\pi} n \cos\left(\frac{2\pi q}{n}\right) . \tag{4.6}$$

Lemma 4.1. *A q-twisted state is stable provided $|q| < \frac{n}{4}$. That is, the Hessian of U at $u^{(q)}$ has zero as a simple eigenvalue, while all other eigenvalues are strictly positive.*

Proof. It follows directly from (4.5) that

$$\frac{\partial^2 U}{\partial u^2} = -2\pi K \cos\bigl(2\pi a\bigr) L \; ,$$

where

$$L = \begin{pmatrix} -2 & 1 & 0 & \dots & \dots & 0 & 1 \\ 1 & -2 & 1 & 0 & \dots & \dots & 0 \\ 0 & 1 & -2 & 1 & 0 & \dots & 0 \\ \vdots & \ddots & \ddots & \ddots & \ddots & \ddots & \vdots \\ 0 & \dots & 0 & 1 & -2 & 1 & 0 \\ 0 & \dots & \dots & 0 & 1 & -2 & 1 \\ 1 & 0 & \dots & \dots & 0 & 1 & -2 \end{pmatrix} \tag{4.7}$$

is the matrix of the discrete Laplacian with periodic boundary conditions. This is a circulant matrix, whose eigenvalues can be computed by discrete Fourier transform. They are given by

$$-\lambda_k^0 = -4\sin^2\biggl(\frac{\pi k}{n}\biggr)\;, \qquad k = 0,\dots,n-1\;. \tag{4.8}$$

The eigenvalues of the Hessian are thus given by

$$-\lambda_k = -8\pi K\cos\biggl(\frac{2\pi q}{n}\biggr)\sin^2\biggl(\frac{\pi k}{n}\biggr)\;. \tag{4.9}$$

If $|q| < n/4$, all λ_k except $\lambda_0 = 0$ are strictly positive. □

The number of stable q-twisted states is equal to

$$N_0 = 1 + 2\max\biggl\{i \in \mathbb{N}_0 \colon i < \frac{n}{4}\biggr\} = 2\biggl\lceil\frac{n}{4}\biggr\rceil - 1\;. \tag{4.10}$$

Remark 4.2. *The proof shows that the case $|q| = \frac{n}{4}$ is degenerate, since the Hessian matrix is the zero matrix, while in the case $|q| > \frac{n}{4}$, the equilibrium is a local maximum of the potential, since all nonzero eigenvalues of the Hessian matrix are strictly negative.*

We still have to examine the effect of the symmetries C_p and I, which are not taken into account by the fundamental domain $\mathcal{D}$.

Lemma 4.3. *For each $q \in \mathbb{Z}/n\mathbb{Z}$, there is exactly one q-twisted state in the fundamental domain $\mathcal{D}$.*

Proof. A representative of $u^{(q)}$ in the hyperplane Σ is given by

$$u^{(q)} = \frac{1}{2n}\bigl(-(n-1)q, -(n-3)q, \dots, (n-3)q, (n-1)q\bigr)^\top\;.$$

Note that this is invariant under the inversion I. Furthermore, since the sum of the first $n-1$ components is $-\frac{(n-1)q}{2n}$, it follows from (3.7) that the corresponding y-coordinates are

$$\begin{aligned} y^{(q)} &= \frac{1}{n}\bigl(-(n-1)q, -(n-2)q, \dots, -q\bigr)^\top \\ &= \frac{1}{n}\bigl(q, 2q, \dots, (n-1)q\bigr)^\top + (q, q, \dots, q)^\top\;. \end{aligned}$$

Consider now the cyclic permutation

$$C_1 u^{(q)} = \frac{1}{2n}\bigl(-(n-3)q, -(n-5)q, \dots, (n-3)q, (n-1)q, -(n-1)q\bigr)^\top\;.$$

The sum of its $n-1$ first components is $\frac{n-1}{2n}q$. Using (3.7), we obtain that its y-coordinates are

$$C_1 y^{(q)} = \frac{1}{n}\bigl(q, 2q, \dots, (n-1)q\bigr)^\top \sim y^{(q)}\;.$$

Since $y^{(q)}$ and $C_1 y^{(q)}$ are related by an integer translation, they correspond to the same point in the fundamental domain $\mathcal{D}$. Cyclic permutations and the inversion being the only candidates for possible other q-twisted states in $\mathcal{D}$, the claim follows. □

4.3 The saddles

Consider now the case where $p = n-1$ of the σ_i are equal to 1, say $\sigma = (1,\dots,1,-1)$. These states have a "jump" between $i = n-1$ and $i = 0$. Other equilibria with the same Morse index can be obtained by cyclic permutation of the coordinates, which amounts to moving the location of the jump.

Lemma 4.4. *If $n \geqslant 5$, equilibria with $\sigma = (1,\dots,1,-1)$ are of the form*

$$u_i^{(r)} = \frac{\hat{q} i}{n} , \qquad i \in \Lambda , \qquad \hat{q} = \frac{rn}{n-2} , \tag{4.11}$$

where $r \in \mathbb{Z} + \frac{1}{2}$ is any half integer satisfying

$$-\frac{n}{4} + \frac{1}{2} < r < \frac{n}{4} - \frac{1}{2} .$$

Proof. According to the discussion of Section 4.1, there are two cases to consider, depending on the value of a. Recall that $a \in [0,1)$ satisfies $\cos(2\pi a) > 0$.

- The first case occurs if $0 \leqslant a < \frac{1}{4}$. Then $\hat{a} = \frac{1}{2} - a$, and Condition (4.2) with $p = n-1$ becomes
$$(n-2)a = \omega - \frac{1}{2} \qquad \Rightarrow \qquad a = \frac{2\omega - 1}{2(n-2)} .$$
Setting $r = \omega - \frac{1}{2}$ yields the expression (4.11) for the equilibrium. The condition $0 \leqslant a < \frac{1}{4}$ becomes
$$\frac{1}{2} \leqslant r < \frac{n}{4} - \frac{1}{2} .$$

- The second case occurs if $\frac{3}{4} < a < 1$. Then $\hat{a} = \frac{3}{2} - a$, and Condition (4.2) with $p = n-1$ becomes
$$(n-2)a = \omega - \frac{3}{2} \qquad \Rightarrow \qquad a = \frac{2\omega - 3}{2(n-2)} .$$
Here it is more convenient to view the state as having a "negative slope". This amounts to replacing a by $a-1$, and setting $r = \omega - n + \frac{1}{2}$ with
$$-\frac{n}{4} + \frac{1}{2} < r \leqslant -\frac{1}{2} ,$$
which yields again the expression (4.11) for the equilibrium. □

Remark 4.5. *In the case $n = 3$, there is no admissible equilibrium with $\sigma = (1,1,-1)$. However, the rôle of 1-saddle is played by the equilibrium with $\sigma = (1,-1,-1)$, which is also of the form (4.11) with $r = \frac{1}{2}$ and $\hat{q} = \frac{3}{2}$. It corresponds to $a = 0$ and $\hat{a} = \frac{1}{2}$. That state is a 1-saddle because a direct computation shows that the eigenvalues of $M(\sigma)$ are -1, 0 and 3. The case $n = 4$ is degenerate, as for the sinks, because then the Hessian matrix is identically zero.*

The value of the potential at the equilibria $u^{(r)}$ is given, according to (4.4), by

$$U(u^{(r)}) = -\frac{K}{2\pi}(n-2)\cos\biggl(2\pi \frac{r}{n-2}\biggr) . \tag{4.12}$$

Proposition 4.6. *For $-\frac{n}{4} + \frac{1}{2} < r < \frac{n}{4} - \frac{1}{2}$, $u^{(r)}$ is a 1-saddle of (1.1), i.e., the Hessian $\frac{\partial^2 U}{\partial u^2}\bigl(u^{(r)}\bigr)$ has one negative eigenvalue, the zero eigenvalue, and $n-2$ positive eigenvalues.*

To prove the proposition, we observe that (4.5) implies that the Hessian matrix of U at these states is given by

$$\frac{\partial^2 U}{\partial u^2}\big(u^{(r)}\big) = -2\pi K \cos\biggl(\frac{2\pi\hat{q}}{n}\biggr) M , \qquad M = D + N , \tag{4.13}$$

where D is the matrix of the discrete Laplacian with Neumann boundary conditions

$$D = \begin{pmatrix} -1 & 1 & 0 & \dots & \dots & \dots & 0 \\ 1 & -2 & 1 & 0 & \dots & \dots & 0 \\ 0 & 1 & -2 & 1 & 0 & \dots & 0 \\ \vdots & \ddots & \ddots & \ddots & \ddots & \ddots & \vdots \\ 0 & \dots & 0 & 1 & -2 & 1 & 0 \\ 0 & \dots & \dots & 0 & 1 & -2 & 1 \\ 0 & \dots & \dots & \dots & 0 & 1 & -1 \end{pmatrix} ,$$

and N is the rank 1 matrix

$$N = \begin{pmatrix} 1 & 0 & \dots & 0 & -1 \\ 0 & 0 & \dots & 0 & 0 \\ \vdots & & & & \vdots \\ 0 & 0 & \dots & 0 & 0 \\ -1 & 0 & \dots & 0 & 1 \end{pmatrix} = \psi\psi^\top , \qquad \psi = \begin{pmatrix} 1 \\ 0 \\ \vdots \\ 0 \\ -1 \end{pmatrix} .$$

The eigenvalues of $-D$ are known to have the form

$$\nu_k^0 = 4\sin^2\biggl(\frac{\pi k}{2n}\biggr) , \qquad k = 0, \dots, n-1 .$$

The corresponding eigenvectors have components

$$\varphi_k^0(i) = \sqrt{\frac{2}{n}} \cos\biggl(\frac{\pi k (i+\frac12)}{n}\biggr) , \qquad i = 0, \dots, n-1$$

for $k \neq 0$, while φ_0^0 is a constant vector. One easily checks that

$$\langle \psi, \varphi_k^0 \rangle = \begin{cases} 0 & \text{if } k \text{ is even} , \\ 2\sqrt{\dfrac{2}{n}} \cos\biggl(\dfrac{\pi k}{2n}\biggr) & \text{if } k \text{ is odd} . \end{cases}$$

The following result is well known in the theory of perturbations by rank 1 linear operators.

Lemma 4.7. *Denote the eigenvalues of $-M$ by ν_k, $k = 0, \dots, n-1$. Then for even k, we have $\nu_k = \nu_k^0$. The odd-numbered eigenvalues of $-M$ satisfy the equation*

$$F(\nu) := \sum_{k \text{ odd}} \frac{\langle \psi, \varphi_k^0 \rangle^2}{\nu_k^0 - \nu} = 1 . \tag{4.14}$$

Proof. If k is even, since $\langle \psi, \varphi_k^0 \rangle = 0$, φ_k^0 is an eigenvector of $-M$ for the same eigenvalue. If ν is an eigenvalue of $-M$ which is not an eigenvalue of $-D$, then the eigenvalue equation can be written

$$\big(-D - \nu\big)\varphi - \langle \psi, \varphi \rangle \psi = 0 , \tag{4.15}$$

so that

$$\varphi = \langle \psi, \varphi \rangle \bigl(-D - \nu\bigr)^{-1} \psi \;.$$

It follows that

$$\langle \psi, \varphi \rangle = \langle \psi, \varphi \rangle \langle \psi, \bigl(-D - \nu\bigr)^{-1} \psi \rangle \;.$$

We must have $\langle \psi, \varphi \rangle \neq 0$, since otherwise, (4.15) would imply that ν is an eigenvalue of $-D$. (Note also that ψ lies in the subspace orthogonal to the span of the φ^0_k with even k, which is invariant under D.) Therefore, we obtain

$$\begin{aligned}
1 &= \langle \psi, \bigl(-D - \nu\bigr)^{-1} \psi \rangle \\
&= \sum_{k \text{ odd}} \langle \psi, \varphi^0_k \rangle \langle \varphi^0_k, \bigl(-D - \nu\bigr)^{-1} \psi \rangle \\
&= \sum_{k \text{ odd}} \langle \psi, \varphi^0_k \rangle \bigl(\nu^0_k - \nu\bigr)^{-1} \langle \varphi^0_k, \psi \rangle \\
&= \sum_{k \text{ odd}} \frac{\langle \psi, \varphi^0_k \rangle^2}{\nu^0_k - \nu} \;,
\end{aligned}$$

from which the claim follows. □

Proof of Proposition 4.6. The function F has poles on the eigenvalues ν^0_k of $-D$ (k odd), and is otherwise strictly increasing. Furthermore, it converges to 0 as $\nu \to \pm\infty$. It follows that (4.14) has exactly one solution in each interval $(\nu^0_{2\ell+1}, \nu^0_{2\ell+3})$ (this is called interlacing), and an additional solution that is smaller than ν^0_1.

Note that

$$\begin{aligned}
\psi^\top N \psi &= 2\psi^\top \psi = 4 \;, \\
\psi^\top D \psi &= -2 \;,
\end{aligned}$$

showing that M has at least one strictly positive eigenvalue. By the interlacing result, there is exactly one such eigenvalue, showing that the smallest eigenvalue ν_1 of $-M$ is strictly negative. The state $u^{(r)}$ is thus indeed a saddle of index 1. To summarize, the odd-numbered eigenvalues satisfy

$$\nu_1 < 0 = \nu^0_0 < \nu^0_1 < \nu_3 < \nu^0_3 < \nu_5 < \nu^0_5 < \dots \;.$$

This shows in particular that the $u^{(r)}$ are indeed 1-saddles. □

One can check that the condition $-\frac{n}{4} + \frac{1}{2} < r < \frac{n}{4} - \frac{1}{2}$ implies that the number N_1 of 1-saddles $u^{(r)}$, having a jump between $i = n-1$ and $i = 0$, is given by

$$N_1 = N_0 - 1 \;,$$

where N_0 is the number of stable q-twisted states, see (4.10).

As before, we also examine the effect of the symmetries C_p and I.

Lemma 4.8. *If $n \neq 4$, then the representatives of $u^{(r)}$, $C_1 u^{(r)}$, ..., $C_{n-1} u^{(r)}$ in the fundamental domain are all different. Therefore, there are exactly n 1-saddles for each admissible r in the fundamental domain.*

Proof. A representative of $u^{(r)}$ in the hyperplane Σ is given by

$$u^{(r)} = \frac{1}{2n}\bigl(-(n-1)\hat{q}, -(n-3)\hat{q}, \dots, (n-3)\hat{q}, (n-1)\hat{q}\bigr)^\top .$$

Note that this is invariant under the inversion I. The sum of the first $n-1$ components being $-\frac{(n-1)\hat{q}}{2n}$, the corresponding y-coordinates are

$$y^{(r)} = \frac{1}{n}\bigl(-(n-1)\hat{q}, -(n-2)\hat{q}, \dots, -\hat{q}\bigr)^\top .$$

Applying the cyclic permutation, we find

$$C_1 u^{(r)} = \frac{1}{2n}\bigl(-(n-3)\hat{q}, \dots, (n-3)\hat{q}, (n-1)\hat{q}, -(n-1)\hat{q}\bigr)^\top .$$

The sum of the first $n-1$ components is now $-\frac{(n-1)\hat{q}}{2n}$, and the corresponding y-coordinates are

$$C_1 y^{(r)} = \frac{1}{n}\bigl(\hat{q}, 2\hat{q}, \dots, (n-1)\hat{q}\bigr)^\top .$$

In a similar manner, we find

$$\begin{aligned}
C_2 y^{(r)} &= \frac{1}{n}\bigl(\hat{q}, 2\hat{q}, \dots, (n-2)\hat{q}, -\hat{q}\bigr)^\top , \\
C_3 y^{(r)} &= \frac{1}{n}\bigl(\hat{q}, 2\hat{q}, \dots, (n-3)\hat{q}, -2\hat{q}, -\hat{q}\bigr)^\top , \\
&\dots \\
C_{n-1} y^{(r)} &= \frac{1}{n}\bigl(\hat{q}, -(n-2)\hat{q}, \dots, -\hat{q}\bigr)^\top .
\end{aligned}$$

We observe that

$$C_p y^{(r)} = y^{(r)} + \bigl(\underbrace{\hat{q}, \dots, \hat{q}}_{n-p \text{ times}}, \underbrace{0, \dots, 0}_{p-1 \text{ times}}\bigr)^\top .$$

We conclude that all n saddles obtained by cyclic permutation of $u^{(r)}$ have different representatives in the fundamental domain, unless $\hat{q}$ is an integer. Since

$$\hat{q} = r\left(1 + \frac{2}{n-2}\right) ,$$

this is the case if and only if $\frac{2}{n-2}$ is an odd integer, which is the case if and only if $n = 4$. □

Remark 4.9. *As remarked before, the case $n = 4$ is degenerate. We already know that the Hessian matrix at the ± 1-twisted states is identically zero in this case. The state $u^{(1/2)}$ is actually identical with $u^{(1)}$, because in the notations of Section 4.1, it corresponds to $a = \hat{a} = \frac{1}{4}$. It may be the case that there are additional constants of motion in this situation.*

Example 4.10. Returning to the case $n = 3$, the list of all equilibria is given in Table 1. They are also shown in Figure 7, to be compared with the contour plot of the potential in Figure 6. Note that the 0-twisted state $u^{(0)}$ communicates with six copies of itself, via six 1-saddles, which are given by two copies each for the three states $u^{(1/2)}$, $C_1 u^{(1/2)}$ and $C_2 u^{(1/2)}$.

In this situation, if the dynamics is described in the fundamental domain, metastable transitions correspond to the system leaving a neighborhood of $u^{(0)}$, and returning to it after passing near one of the 1-saddles. By contrast, if the system is viewed as evolving in the whole hyperplane Σ, the different copies of $u^{(0)}$ are no longer considered to be all the same state, and the dynamics resembles a random walk between these copies (see also Remark 3.3).

Equilibrium	(u_0, u_1)	(y_0, y_1)
$u^{(0)}$	$(0,0)$	$(0,0)$
$u^{(1)}$	$(\frac{1}{3}, -\frac{1}{3})$	$(\frac{1}{3}, -\frac{1}{3})$
$u^{(-1)}$	$(-\frac{1}{3}, \frac{1}{3})$	$(-\frac{1}{3}, \frac{1}{3})$
$u^{(1/2)}$	$(\frac{1}{6}, -\frac{1}{3})$	$(0, -\frac{1}{2})$
$C_1 u^{(1/2)}$	$(-\frac{1}{3}, \frac{1}{6})$	$(-\frac{1}{2}, 0)$
$C_2 u^{(1/2)}$	$(-\frac{1}{6}, -\frac{1}{6})$	$(-\frac{1}{2}, -\frac{1}{2})$

Table 1: List of all equilibria in the fundamental domain $\mathcal{D}$ in the case $n = 3$, with their u and y-coordinates.

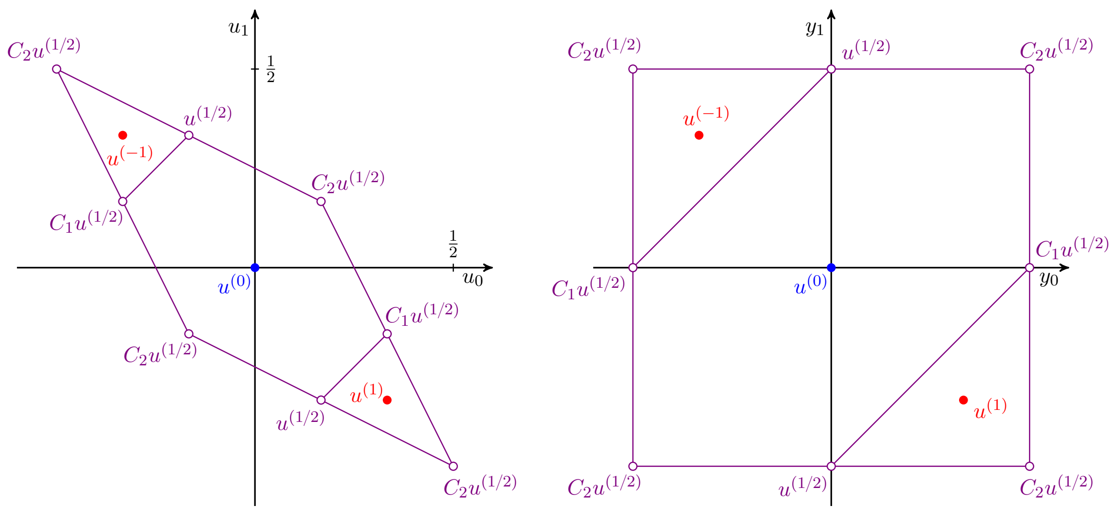

Figure 7: Equilibria in the fundamental domain, in the case $n = 3$. They are shown in u and y-coordinates, with sinks in blue, local maxima in red, and 1-saddles in violet. Points on opposite sides and corners of the fundamental domain are identified. The violet lines indicate the stable/unstable manifolds of the 1-saddles (it follows from (3.6) that the potential is constant on these lines), and part of them are domain boundaries.

4.4 Other equilibria

In order to determine the metastable hierarchy, it will be useful to know exactly how many equilibria have Morse index 0 or 1. Recall that we have introduced the integer

$$p = \#\{i \in \Lambda \colon a_i = a\} = \#\{i \in \Lambda \colon \sigma_i = 1\} \in \{1, \dots, n\} .$$

The case $p = n$ corresponds to q-twisted states, which have either Morse index 0 (sinks), or Morse index n (local maxima of the potential), or are degenerate, in the special case $|q| = \frac{n}{4}$. The case $p = n - 1$ corresponds to 1-saddles.

It thus remains to consider the cases where $1 \leqslant p \leqslant n - 2$. The following result shows that these equilibria cannot have Morse index 0 or 1, and therefore are not important for the metastable dynamics of the system.

Lemma 4.11. *Assume $n \geqslant 5$. Then any equilibrium point with $1 \leqslant p \leqslant n-2$, that is, with at least two σ_i equal to -1, is a saddle of Morse index 2 at least.*

Proof. Since $p \leqslant n-2$, we may assume that $\sigma_0 = 1$. Let $(e_0, \dots, e_{n-1})$ be the canonical basis of $\mathbb{R}^\Lambda$. Our aim is to construct vectors $\hat{e}_1$ and $\hat{e}_2$, orthogonal to each other, and such that the restriction of $M(\sigma)$ to the subspace spanned by these vectors is negative definite.

Let i be the smallest $i \geqslant 1$ such that $\sigma_i = -1$. We first consider the case where $\sigma_{i+1} = -1$. Then the restriction of $M(\sigma)$ to $\operatorname{span}(e_{i-1}, e_i, e_{i+1}, e_{i+2})$ is given by

$$\widehat{M} = \begin{pmatrix} \sigma_{i-2} - 1 & -1 & 0 & 0 \\ -1 & 0 & 1 & 0 \\ 0 & 1 & -2 & 1 \\ 0 & 0 & 1 & \sigma_{i+2} - 1 \end{pmatrix} .$$

Consider the vectors

$$\hat{e}_1 = e_{i-1} + 2e_i \;, \qquad \hat{e}_2 = -e_{i+1} + e_{i+2} \;.$$

Computing $\langle \hat{e}_p, \widehat{M} \hat{e}_q \rangle$ for $p, q \in \{1, 2\}$, one obtains that the restriction of $M(\sigma)$ to $\operatorname{span}(\hat{e}_1, \hat{e}_2)$ is given by

$$\begin{pmatrix} \sigma_{i-2} - 3 & -2 \\ -2 & \sigma_{i+2} - 5 \end{pmatrix} .$$

One easily checks that this matrix is negative definite, for any values of $\sigma_{i-2}, \sigma_{i+2} \in \{-1, 1\}$.

Consider now the case $\sigma_{i+1} = 1$. Let $j \geqslant i+2$ be the smallest j such that $\sigma_{j-1} = 1$ and $\sigma_j = -1$. Then the restriction of $M(\sigma)$ to $\operatorname{span}(e_i, e_{i+1}, e_j, e_{j+1})$ is given by

$$\widehat{M} = \begin{pmatrix} 0 & 1 & 0 & 0 \\ 1 & 0 & M_{i+1,j} & 0 \\ 0 & M_{i+1,j} & 0 & 1 \\ 0 & 0 & 1 & \sigma_{j+1} - 1 \end{pmatrix} ,$$

where $M_{i+1,j} = -1$ if $j = i+2$, and 0 otherwise. Consider the vectors

$$\hat{e}_1 = e_i - e_{i+1} \;, \qquad \hat{e}_2 = e_j + e_{j+1} \;.$$

The restriction of $M(\sigma)$ to $\operatorname{span}(\hat{e}_1, \hat{e}_2)$ is given by

$$\begin{pmatrix} -2 & -M_{i+1,j} \\ -M_{i+1,j} & \sigma_{j+1} - 3 \end{pmatrix} .$$

One again easily checks that this matrix is negative definite, for any values of $\sigma_{j+1} \in \{-1, 1\}$ and $M_{i+1,j} \in \{-1, 0\}$. □

4.5 Relevant saddles and metastable hierarchy

In this subsection, we identify the relevant saddles between the q-twisted states, as defined in Section 2.

Proposition 4.12. *For any q such that $1 \leqslant |q| < \frac{n}{4}$, the set of relevant saddles between the sink $u^{(q)}$ and the set $\{u^{(-|q|+1)}, u^{(-|q|+2)}, \dots, u^{(|q|-1)}\}$ is*

$$\left\{ C_p u^{(|q|-1/2)}, C_p u^{(-|q|+1/2)} \colon 0 \leqslant p \leqslant n-1 \right\} ,$$

where we recall that C_p denotes the cyclic permutation defined in (3.2).

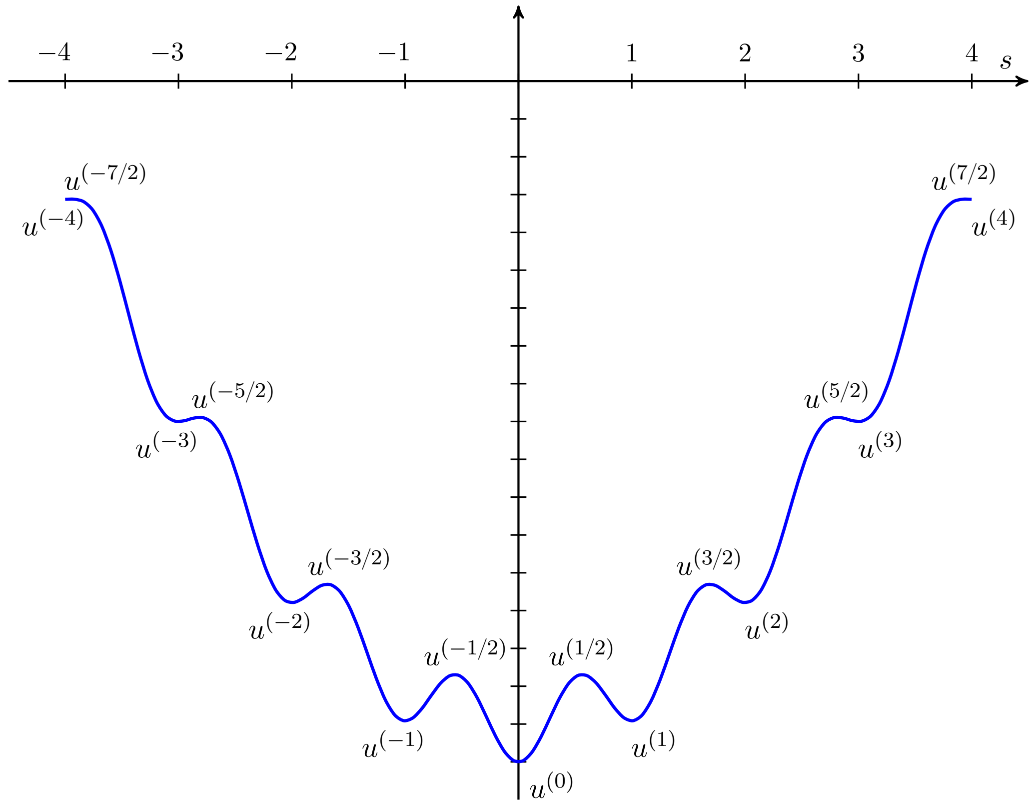

Figure 8: The potential $U(u(s))$ for $n = 18$ and $K = 2\pi$. The local minima are located at the q-twisted states $u(s) = u^{(q)}$, while the local maxima are on the 1-saddles $u(\hat{s}_q) = u^{(q+1/2)}$.

Proof. We want to show that any minimal path from $u^{(q)}$ to $\{u^{(-|q|+1)}, u^{(-|q|+2)}, \dots, u^{(|q|-1)}\}$, as defined in Section 2 above, contains at least one of the points of the given list as its hightest point. Note that (4.12) implies that the value of U is the same at all points in the list.

Let $m = \max\{q \in \mathbb{N}_0 \colon q < \frac{n}{4}\}$, so that the sinks are parametrized by $q \in \{-m, \dots, m\}$. We define a curve $u : [-m, m] \to (\mathbb{R}/\mathbb{Z})^\Lambda$ by

$$u_i(s) = \frac{s}{n} i \,, \qquad s \in [-m, m] \,, \qquad i \in \Lambda \,.$$

Note that for any $q \in [-m, m]$, we have

$$u(s) = u^{(q)} \quad \Leftrightarrow \quad s = q \,,$$

while

$$u(s) = u^{(q+\frac{1}{2})} \quad \Leftrightarrow \quad s = \hat{s}_q := \left(q + \frac{1}{2}\right) \frac{n}{n-2} \,.$$

In other terms, the curve $\{u(s)\}_{s \in [-m,m]}$ visits the equilibria $u^{(-m)}$, $u^{(-m+1/2)}$, $u^{(-m+1)}$, $\dots$ up to $u^{(m)}$ in this order. By (4.3), the potential along this curve is given by

$$U(u(s)) = -\frac{K}{2\pi} \left[(n-1) \cos\left(2\pi \frac{s}{n}\right) + \cos\left(2\pi \frac{n-1}{n}\right) s \right] .$$

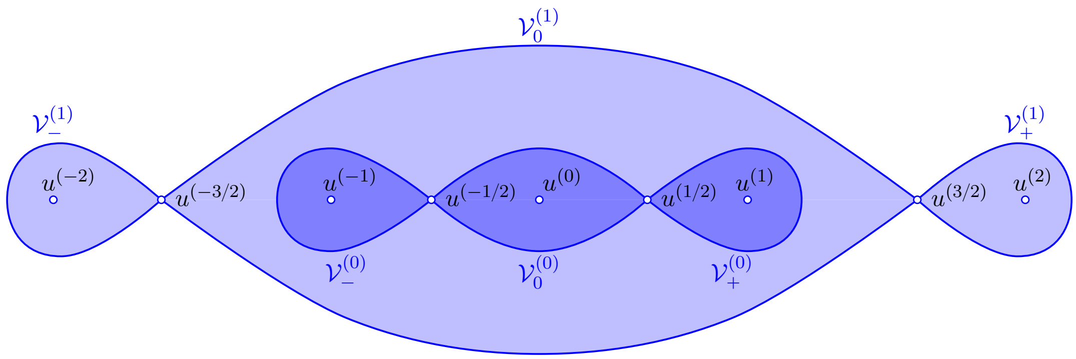

Figure 9: Construction of the metastable hierarchy. The set $\mathcal{V}^{(0)} = \mathcal{V}_-^{(0)} \cup \mathcal{V}_0^{(0)} \cup \mathcal{V}_+^{(0)}$ is the union of the open valleys $\mathcal{OV}(u^{(1/2)})$ and $\mathcal{OV}(u^{(-1/2)})$, which overlap in the central component. Similarly, the set $\mathcal{V}^{(1)}$ is the union of the open valleys $\mathcal{OV}(u^{(3/2)})$ and $\mathcal{OV}(u^{(-3/2)})$.

The derivative of this function is

$$\begin{aligned}\frac{\mathrm{d}}{\mathrm{d}s}U(u(s)) &= K\frac{n-1}{n}\left[\sin\left(2\pi\frac{s}{n}\right) + \sin\left(2\pi\frac{n-1}{n}s\right)\right] \\ &= 2K\frac{n-1}{n}\sin(2\pi s)\cos\left(2\pi\frac{n-2}{n}s\right) ,\end{aligned}$$

where we have used the sum-product formula $\sin\alpha + \sin\beta = 2\sin(\frac{\alpha+\beta}{2})\cos(\frac{\alpha-\beta}{2})$. It is straightforward to check that this derivative in positive on the intervals $(q, \hat{s}_q)$, and negative on the intervals $(\hat{s}_q, q+1)$.

The proof now follows by induction on $|q|$. By symmetry, we may restrict the discussion to the case $q > 0$ and $p = 0$. In the base case $q = 1$, the restricted curve $\{u(1-s)\}_{s\in[0,1]}$ provides a path from $u^{(1)}$ to $u^{(0)}$, containing the saddle $u^{(1/2)}$ as its highest point. Furthermore, it is known that since all critical points are non-degenerate, any minimal path from $u^{(1)}$ to $u^{(0)}$ has to contain a saddle of index 1. Since $u^{(1/2)}$ and $u^{(-1/2)}$ are the lowest 1-saddles, the path is minimal, and the claim follows for $q = 1$.

To proceed, we need some topological properties of the potential landscape (see for instance [8, Section 2.1]). Let $\hat{u}$ be a 1-saddle, and define its *closed valley* and *open valley*, respectively, by

$$\begin{aligned}\mathcal{CV}(\hat{u}) &= \left\{u \colon \overline{V}(u,\hat{u}) \leqslant U(\hat{u})\right\} , \\ \mathcal{OV}(\hat{u}) &= \left\{u \in \mathcal{CV}(\hat{u}) \colon U(u) < U(\hat{u})\right\} .\end{aligned}$$

If the potential is of class $\mathcal{C}^2$ and $\hat{u}$ is non-degenerate, then $\mathcal{OV}(\hat{u})$ has at most two connected components, containing the two parts of the one-dimensional unstable manifold of $\hat{u}$. Furthermore, $\mathcal{CV}(\hat{u})$ is the closure of $\mathcal{OV}(\hat{u})$, and is path-connected. Intuitively, if $\mathcal{OV}(\hat{u})$ has two connected components, these components meet at the saddle point $\hat{u}$, and only there.

Returning to our particular problem, we set

$$\mathcal{V}^{(0)} = \mathcal{OV}(u^{(1/2)}) \bigcup \mathcal{OV}(u^{(-1/2)}) .$$

This set has exactly three connected components: the component $\mathcal{V}_+^{(0)}$ containing $u^{(1)}$, the component $\mathcal{V}_-^{(0)}$ containing $u^{(-1)}$, and the component $\mathcal{V}_0^{(0)}$ containing $u^{(0)}$, which is also the intersection of the open valleys $\mathcal{OV}(u^{(1/2)})$ and $\mathcal{OV}(u^{(-1/2)})$, see Figure 9. We claim that each component contains only one sink. Indeed, if one component contained two different sinks, it would have to contain a 1-saddle as well. But this is not possible, since all 1-saddles have height $U(u^{(1/2)})$ at least, while points in the components are lower by construction.

We now assume by induction that the claim is true for a given $q < \frac{n}{4} - 1$, and that the set

$$\mathcal{V}^{(q-1)} = \mathcal{OV}(u^{(q-1/2)}) \bigcup \mathcal{OV}(u^{(-q+1/2)}) \tag{4.16}$$

has exactly three connected component. The components containing $u^{(q)}$ and $u^{(-q)}$ contain each exactly one sink, while the remaining component $\mathcal{V}_0^{(q-1)}$ contains the sinks $u^{(-q+1)}, \dots u^{(q-1)}$ and the saddles $u^{(-q+3/2)}, \dots, u^{(q-3/2)}$, and no other sinks or 1-saddles.

The induction step proceeds as follows. The restriction $\{u(q+1-s)\}_{s\in[0,1]}$ provides a path from $u^{(q+1)}$ to $u^{(q)}$. Now assume by contradiction that there is another path from $u^{(q+1)}$ to a sink $u^{(q')}$, with $-q \leqslant q' \leqslant q$, whose highest point is below $U(u^{(q+1/2)})$. This highest point must be one of the saddles $u^{(-q+1/2)}, \dots, u^{(q-1/2)}$, since these are the only saddles lower than $u^{(q+1/2)}$. Call this saddle $u^{(r)}$. But this would mean that $u^{(q+1)}$ belongs to the open valley of $u^{(r)}$, which lies in $\mathcal{V}^{(q-1)}$. This contradicts the fact that $\mathcal{V}^{(q-1)}$ does not contain $u^{(q+1)}$. We conclude that the above path from $u^{(q+1)}$ to $u^{(q)}$ is minimal.

Furthermore, this shows that the open valley $\mathcal{OV}(u^{(q+1/2)})$ has two connected components, one of them containing $u^{(q+1)}$, and the other one containing $u^{(q)}$. The latter will in fact contain all sinks $u^{(-q)}, \dots, u^{(q)}$ by the induction hypothesis. A similar argument holds for $u^{(-q-1/2)}$, which implies that $\mathcal{V}^{(q)}$ has a similar decomposition as (4.16). The induction step is thus complete. □

The next result provides information on the metastable hierarchy.

Proposition 4.13. *The potential difference*

$$\Delta U(q) = U(u^{(q+1/2)}) - U(u^{(q+1)})$$

is a decreasing function of q *for* $0 \leqslant q \leqslant \frac{n}{4} - 1$.

Proof. Using (4.6) and (4.12), we get

$$\begin{aligned} \frac{2\pi}{K} \Delta U(q) &= n \cos\biggl(\frac{2\pi(q+1)}{n}\biggr) - (n-2)\cos\biggl(\pi\frac{2q+1}{n-2}\biggr) \\ &=: n\cos(\beta) - (n-2)\cos(\alpha) \;. \end{aligned}$$

This expression is well-defined for any $q \in \mathbb{R}$. We can thus compute its derivative with respect to q, to obtain

$$\frac{1}{K}\frac{\mathrm{d}}{\mathrm{d}q}\Delta U(q) = \sin\alpha - \sin\beta = 2\sin\frac{\alpha-\beta}{2}\cos\frac{\alpha+\beta}{2} \;.$$

The difference

$$\alpha - \beta = -\pi\frac{n-4(q+1)}{n(n-2)}$$

belongs to $(-\pi, 0)$ for $q + 1 < 4n$, while the sum $\alpha + \beta$ is strictly positive. Therefore, the q-derivative of $\Delta U(q)$ is strictly negative, that is, $q \mapsto \Delta U(q)$ is decreasing. □

This result shows that if only sinks with $q \geqslant 0$ were present, we would have a clear metastable hierarchy $u^{(0)} \prec u^{(1)} \prec u^{(2)} \prec \dots$. The existence of the $q \mapsto -q$ symmetry makes the situation slightly degenerate, however, and we will have to examine the consequences of that.

5 Transition times

In this section, we estimate the time separating metastable transitions between various q-twisted states, or sets of q-twisted states. Certain expected transition times, between a q-twisted state and the set $\{u^{(-|q|+1)}, \dots, u^{(|q|-1)}\}$ of more stable states is directly obtained by applying the Eyring–Kramers relation (2.2) to our situation. For more general transitions, computations are more involved.

5.1 Preliminary computations

A central quantity governing expected transition times is the potential difference

$$H_q = U(u^{(q-1/2)}) - U(u^{(q)}) \;, \qquad 1 \leqslant q < \frac{n}{4} \;.$$

For negative q, we set $H_q = H_{-q}$. The potential difference

$$\bar{H}_q = U(u^{(q+1/2)}) - U(u^{(q)}) \;, \qquad 0 \leqslant q < \frac{n}{4}$$

plays a role in transitions to less stable states. Again, for negative q, we set $\bar{H}_q = \bar{H}_{-q}$. While (4.6) and (4.12) provide explicit expressions for these quantities, it is useful to understand their behavior for $|q| \ll n$, as described by the following estimate.

Lemma 5.1. *For fixed* q *and* n *large, one has*

$$\begin{aligned} H_q &= \frac{K}{\pi} - \biggl(q - \frac{1}{4}\biggr)\frac{K\pi}{n} + \mathcal{O}\bigl(n^{-2}\bigr) \;, \qquad 1 \leqslant q \ll n \;, \\ \bar{H}_q &= \frac{K}{\pi} + \biggl(q + \frac{1}{4}\biggr)\frac{K\pi}{n} + \mathcal{O}\bigl(n^{-2}\bigr) \;, \qquad 0 \leqslant q \ll n \;. \end{aligned} \tag{5.1}$$

Proof. The values of $\bar{H}_0$ and H_1 are obtained by a direct Taylor expansion, using (4.6) and (4.12). For any $0 \leqslant q < \frac{n}{4}$, (4.6), (4.12), and sum-product formulas yield

$$\begin{aligned} U(u^{(q+1)}) - U(u^{(q)}) &= \frac{Kn}{\pi}\sin\biggl(\frac{\pi}{n}\biggr)\sin\biggl(\frac{\pi(2q+1)}{n}\biggr) = (2q+1)\frac{K\pi}{n} + \mathcal{O}\bigl(n^{-3}\bigr) \;, \\ U(u^{(q+3/2)}) - U(u^{(q+1/2)}) &= \frac{K(n-2)}{\pi}\sin\biggl(\frac{\pi}{n-2}\biggr)\sin\biggl(\frac{2\pi(q+1)}{n-2}\biggr) \\ &= 2(q+1)\frac{K\pi}{n} + \mathcal{O}\bigl(n^{-2}\bigr) \;. \end{aligned}$$

The result then follows by induction on q, using

$$\bar{H}_{q+1} = \bar{H}_q + U(u^{(q+1)}) - U(u^{(q)}) - \bigl[U(u^{(q+1)}) - U(u^{(q)})\bigr] \;,$$

and a similar relation between H_{q+1} and H_q. □

Another important quantity is the product of eigenvalues appearing in the prefactor in the Eyring–Kramers law (2.2). The eigenvalues λ_k at the sink $u^{(q)}$ can be written, by (4.9), as

$$\lambda_k = 2\pi K \cos\biggl(\frac{2\pi(q+1)}{n}\biggr)\lambda_k^0 \;, \qquad \lambda_k^0 = 4\sin^2\biggl(\frac{\pi k}{n}\biggr) \;. \tag{5.2}$$

Recall from (4.8) that the λ_k^0 are also the eigenvalues of the discrete Laplacian with periodic boundary conditions. The eigenvalues μ_k at the saddles are given by

$$\mu_k = 2\pi K \cos\left(\frac{2\pi\hat{q}}{n}\right)\nu_k \;, \qquad \hat{q} = \left(q + \frac{1}{2}\right)\frac{n}{n-2} \;, \tag{5.3}$$

where the ν_k are the eigenvalues of $-M$ (cf. (4.13)). Combining (5.2) and (5.3), we get

$$\frac{|\mu_1|\mu_2\dots\mu_{n-1}}{\lambda_1\dots\lambda_{n-1}} = \left(\frac{\cos\left(\frac{2\pi\hat{q}}{n}\right)}{\cos\left(\frac{2\pi(q+1)}{n}\right)}\right)^n \frac{|\nu_1|\dots\nu_{n-1}}{\lambda_1^0\dots\lambda_{n-1}^0} \;. \tag{5.4}$$

Taking logarithms and expanding, we have

$$\begin{aligned}\log\left(\frac{\cos\left(\frac{2\pi\hat{q}}{n}\right)}{\cos\left(\frac{2\pi(q+1)}{n}\right)}\right)^n &= n\log\frac{1-\frac{2\pi^2\hat{q}^2}{n^2}+\mathcal{O}(n^{-4})}{1-\frac{2\pi^2(q+1)^2}{n^2}+\mathcal{O}(n^{-4})} \\ &= \frac{2\pi^2}{n}((q+1)^2-\hat{q}^2)+\mathcal{O}\big(n^3\big) \\ &= \frac{2\pi^2}{n}\left(q+\frac{3}{4}\right)+\mathcal{O}\big(n^{-2}\big) \;.\end{aligned}$$

We conclude that

$$\left(\frac{\cos\left(\frac{2\pi(q+1)}{n}\right)}{\cos\left(\frac{2\pi\hat{q}}{n}\right)}\right)^n = 1+\frac{\pi^2(4q+3)}{2n}+\mathcal{O}\big(n^{-2}\big) \;. \tag{5.5}$$

In fact, the error for large but finite n has order $1/n$, and has been computed above. On the other hand, the second factor in (5.4) is described by the following result.

Proposition 5.2. *We have the exact relation*

$$\frac{\nu_1\dots\nu_{n-1}}{\lambda_1^0\dots\lambda_{n-1}^0} = -1+\frac{2}{n} \;. \tag{5.6}$$

Proof. Let L be the matrix (4.7) of the discrete Laplacian with periodic boundary conditions. We observe that $D = L + N$. The λ_k^0 are eigenvalues of $-L$, while the ν_k are eigenvalues of $-M = -D - N = -L - 2N$.

To avoid problems due to the zero eigenvalues, we introduce for $\varepsilon \in \mathbb{R}$ the quantity

$$r(\varepsilon) = \frac{\det(\varepsilon\mathbb{1}-M)}{\det(\varepsilon\mathbb{1}-L)} = \frac{(\varepsilon+\nu_0)(\varepsilon+\nu_1)\dots(\varepsilon+\nu_{n-1})}{(\varepsilon+\lambda_0^0)(\varepsilon+\lambda_1^0)\dots(\varepsilon+\lambda_{n-1}^0)} \;.$$

This function is well-defined whenever ε is not an eigenvalue of L. Moreover, since $\nu_0 = \lambda_0^0 = 0$, we have

$$\frac{\nu_1\dots\nu_{n-1}}{\lambda_1^0\dots\lambda_{n-1}^0} = \lim_{\varepsilon\to 0} r(\varepsilon) \;. \tag{5.7}$$

Now we observe that we can write $r(\varepsilon)$ as a Fredholm determinant

$$\begin{aligned}r(\varepsilon) &= \det\big[(\varepsilon\mathbb{1}-M)(\varepsilon\mathbb{1}-L)^{-1}\big] \\ &= \det\big[\mathbb{1}-2N(\varepsilon\mathbb{1}-L)^{-1}\big] \;.\end{aligned}$$

The inverse of $\varepsilon\mathbb{1}-L$ can be written as

$$(\varepsilon\mathbb{1}-L)^{-1} = \sum_{k=0}^{n-1}\frac{1}{\varepsilon+\lambda_k^0}\Pi_k \;,$$

where Π_k is the projector on the eigenspace associated with λ_k^0, given by

$$\Pi_k = \eta_k \bar{\eta}_k^\top \;, \qquad \eta_k^\top = \frac{1}{\sqrt{n}} \begin{pmatrix} 1 & \varpi^k & \varpi^{2k} & \dots & \varpi^{(n-1)k} \end{pmatrix} , \qquad \varpi = \mathrm{e}^{\mathrm{i}\,2\pi/n} \;.$$

Note that all λ_k^0 except $\lambda_0^0 = 0$ and $\lambda_{n/2}^0 = 4$ (if n is even) have multiplicity 2, so that the choice of the Π_k is not unique, but the above choice is a valid one. Since

$$\langle \psi, \eta_k \rangle = \frac{1 - \varpi^{-k}}{\sqrt{n}} \;,$$

it follows that

$$N(\varepsilon \mathbb{1} - L)^{-1} = \sum_{k=0}^{n-1} \frac{1}{\varepsilon + \lambda_k^0} \langle \psi, \eta_k \rangle \psi \eta_k^\top = \begin{pmatrix} a_1 & a_2 & \dots & a_n \\ 0 & 0 & \dots & 0 \\ \vdots & & & \vdots \\ 0 & 0 & \dots & 0 \\ -a_1 & -a_2 & \dots & -a_n \end{pmatrix} ,$$

where

$$a_j = \frac{1}{n} \sum_{k=0}^{n-1} \frac{1}{\varepsilon + \lambda_k^0} (1 - \varpi^k) \varpi^{k(1-j)} \;.$$

In particular, for $j = 1$, grouping the summands k and $n - k$ one obtains

$$a_1 = \frac{1}{2n} \sum_{k=1}^{n-1} \frac{\lambda_k^0}{\varepsilon + \lambda_k^0} \;.$$

A similar computation shows that $a_n = -a_1$. Now we note that

$$\begin{aligned} r(\varepsilon) = \det\bigl[\mathbb{1} - 2N(\varepsilon \mathbb{1} - L)^{-1}\bigr] &= \begin{vmatrix} 1 - 2a_1 & -2a_2 & \dots & -2a_{n-1} & -2a_n \\ 0 & 1 & & 0 & 0 \\ \vdots & & \ddots & & \vdots \\ 0 & 0 & & 1 & 0 \\ 2a_1 & 2a_2 & \dots & 2a_{n-1} & 1 + 2a_n \end{vmatrix} \\ &= (1 - 2a_1)(1 + 2a_n) - 4a_1 a_n \\ &= 1 - 2a_1 + 2a_n \\ &= 1 - 4a_1 \;. \end{aligned}$$

As ε tends to 0, a_1 converges to $\frac{n-1}{2n}$. Substituting in (5.7) yields the result. □

The last missing piece in order to determine the prefactor in the Eyring–Kramers law is the behavior of ν_1. This is described by the following result.

Proposition 5.3. *The negative eigenvalue ν_1 of $-M$ satisfies*

$$-\frac{4}{3} \leqslant \nu_1 \leqslant -\frac{4}{3} + \frac{1}{3^{n-3}} \;. \tag{5.8}$$

Proof. Consider the subspace $E = \{u \in (\mathbb{R}/\mathbb{Z})^\Lambda \colon u_i = -u_{n-1-i} \forall i \in \{0,\dots,n-1\}\}$. This subspace has dimension $m = n/2$ if n is even, and $m = (n-1)/2$ if n is odd. One easily checks that it is invariant under the matrix M. We claim that the eigenvector v_1 corresponding to ν_1 belongs to E.

A basis of E is given by $(\hat e_0,\dots,\hat e_{m-1}) = (e_0 - e_{n-1}, e_1 - e_{n-2},\dots,e_{m-1}-e_{n-m})$. The form $\widehat M$ of M in this basis is slightly different depending on the parity of n. We consider first the case where n is even. Then

$$\widehat M = \begin{pmatrix} 1 & 1 & 0 & \dots & \dots & 0 & 0 \\ 1 & -2 & 1 & 0 & \dots & \dots & 0 \\ 0 & 1 & -2 & 1 & 0 & \dots & 0 \\ \vdots & \ddots & \ddots & \ddots & \ddots & \ddots & \vdots \\ 0 & \dots & 0 & 1 & -2 & 1 & 0 \\ 0 & \dots & \dots & 0 & 1 & -2 & 1 \\ 0 & 0 & \dots & \dots & 0 & 1 & -3 \end{pmatrix} .$$

Observe that the vector

$$v = \Bigl(1, \frac13, \frac19, \dots, \frac{1}{3^{m-1}}\Bigr)^\top$$

satisfies

$$\widehat M v = \frac43 \Bigl(v - \frac{1}{3^{m-1}} \hat e_{m-1}\Bigr) .$$

As $m \to \infty$, this reduces to $\widehat M v = \frac43 v$, suggesting that $-\widehat M$ has an eigenvalue close to $-\frac43$. To prove this, we consider the matrix

$$\widetilde M = \widehat M + \frac43 \hat e_{m-1} \hat e_{m-1}^\top .$$

This matrix differs from $\widehat M$ only in the bottom right element, which has value $-\frac53$ instead of -3. It satisfies $\widetilde M v = \frac43 v$, and therefore admits $\frac43$ as an eigenvalue. Observe that $\widetilde M$ is a rank-1 perturbation of the discrete Laplacian with periodic boundary conditions L, namely

$$\widetilde M = L + \tilde\psi \tilde\psi^\top , \qquad \tilde\psi^\top = \begin{pmatrix} \sqrt3 & 0 & \dots & 0 & -\frac{1}{\sqrt3} \end{pmatrix} .$$

We claim that $-\frac43$ is the only negative eigenvalue of $-\widetilde M$. To show this, we proceed similarly to the proof of Lemma 4.7. Let $\tilde\mu$ be an eigenvalue of $-\widetilde M$. This means that there exists a vector $\tilde\varphi \neq 0$ such that

$$\bigl(L + \tilde\psi\tilde\psi^\top + \tilde\mu\bigr)\tilde\varphi = 0 ,$$

and therefore

$$\bigl(L + \tilde\mu\bigr)\tilde\varphi = -\langle \tilde\psi, \tilde\varphi\rangle \tilde\psi . \tag{5.9}$$

If $\tilde\mu$ is an eigenvalue of $-L$, then $\tilde\mu \geqslant 0$, and the claim is proved. We thus assume that $\tilde\mu$ is not an eigenvalue of $-L$. Then

$$\tilde\varphi = -\langle \tilde\psi, \tilde\varphi\rangle \bigl(L + \tilde\mu\bigr)^{-1} \tilde\psi . \tag{5.10}$$

We must have $\langle \tilde\psi, \tilde\varphi\rangle \neq 0$, since otherwise (5.9) would imply that $\tilde\mu$ is an eigenvalue of $-L$. Taking the inner product of (5.10) with $\tilde\psi$, and dividing by $\langle \tilde\psi, \tilde\varphi\rangle$, we obtain

$$-1 = \langle \tilde\psi, (L+\tilde\mu)^{-1}\tilde\psi\rangle = \sum_k \frac{\langle \tilde\psi, \varphi^0_k\rangle^2}{\tilde\mu - \lambda^0_k} =: F_1(\tilde\mu) .$$

Here the sum ranges over the eigenvalues λ_k^0 of $-L$, with associated normalized eigenvectors φ_k^0. The function F_1 has poles on the eigenvalues of $-L$, which are non-negative, and is otherwise strictly decreasing. Therefore, the equation $F_1(\tilde{\mu})$ can have only one strictly negative eigenvalue, and the claim is proved.

Consider now the eigenvalue equation $(\widehat{M} + \nu_1)\varphi_1 = 0$, which is equivalent to

$$\big(\widetilde{M} + \nu_1\big)\varphi_1 = \frac{4}{3}\langle \hat{e}_{m-1}, \varphi_1\rangle \hat{e}_{m-1} \;.$$

If $\nu_1 = \tilde{\mu}_1 = -\frac{4}{3}$, the proposition is proved. Otherwise, ν_1 is not an eigenvalue of $\widetilde{M}$, and $\langle \hat{e}_{m-1}, \varphi_1\rangle \neq 0$, so that we get

$$\frac{3}{4} = \langle \hat{e}_{m-1}, (\widetilde{M} + \nu_1)^{-1}\hat{e}_{m-1}\rangle = \sum_k \frac{\langle \hat{e}_{m-1}, \tilde{\varphi}_k\rangle^2}{\nu_1 - \tilde{\mu}_k} \;,$$

where the sum ranges over the eigenvalues $\tilde{\mu}_k$ of $\widetilde{M}$, with associated normalized eigenvectors $\tilde{\varphi}_k$. Isolating the term $k = 1$, we obtain

$$\nu_1 + \frac{4}{3} = \frac{\langle \tilde{\varphi}_1, \hat{e}_{m-1}\rangle^2}{\frac{3}{4} + S} \;, \qquad S = \sum_{k\neq 1} \frac{\langle \hat{e}_{m-1}, \tilde{\varphi}_k\rangle^2}{\tilde{\mu}_k - \nu_1} \;.$$

Since $\nu_1 < 0$ and all $\tilde{\mu}_k$ except $\tilde{\mu}_1$ are positive, S is positive. Furthermore, since $\tilde{\varphi}_1 = v/\|v\|$ we have

$$\langle \tilde{\varphi}_1, \hat{e}_{m-1}\rangle^2 = \frac{\langle v, \hat{e}_{m-1}\rangle^2}{\|v\|^2} = \frac{9}{8(1-9^{-m})3^{2m-2}} \leqslant \frac{1}{4\cdot 3^{2m-2}} \;.$$

This yields the upper bound on ν_1, using the fact that $2m \geqslant n - 2$.

It remains to consider the case where M is odd. Then

$$\widehat{M} = \begin{pmatrix} 1 & 1 & 0 & \dots & \dots & 0 & 0 \\ 1 & -2 & 1 & 0 & \dots & \dots & 0 \\ 0 & 1 & -2 & 1 & 0 & \dots & 0 \\ \vdots & \ddots & \ddots & \ddots & \ddots & \ddots & \vdots \\ 0 & \dots & 0 & 1 & -2 & 1 & 0 \\ 0 & \dots & \dots & 0 & 1 & -2 & 1 \\ 0 & 0 & \dots & \dots & 0 & 1 & -2 \end{pmatrix} = \widetilde{M} - \frac{1}{3}\hat{e}_{m-1}\hat{e}_{m-1}^{\top} \;.$$

Then a completely analogous argument shows that $\nu_1 \leqslant -\frac{4}{3} + \frac{1}{4}3^{3-2m} = -\frac{4}{3} + \frac{1}{4}3^{4-n}$, which is smaller than the stated bound. $\square$

5.2 Expected transition time from less stable to more stable states

The following result follows essentially from [11], except for the fact that the potential U has the point symmetry $U(-u) = U(u)$. A generalization of the results from [11] to potentials invariant under a discrete symmetry group has been obtained in [4] for continuous-time Markov chains on a finite set, and in [16] for stochastic differential equations. See also [5] for an application to a discretized Allen–Cahn equation with conserved total mass.

Below, we will write

$$\mathcal{M}_q = \{u^{(-q)}, u^{(-q+1)}, \dots, u^{(q)}\}$$

for the qth metastable set, while the distance between two discrete sets $A, B \subset (\mathbb{R}/\mathbb{Z})^\Lambda$ is given by $\operatorname{dist}(A, B) = \inf_{a\in A, b\in B} \|a - b\|$.

Theorem 5.4. *Fix q such that $0 \leqslant q < \frac{n}{4}$, $\delta > 0$, and let*

$$\tau_{\mathcal{M}_q} = \inf\Big\{t > 0\colon \operatorname{dist}\big(u_t, \mathcal{M}_q\big) < \delta\Big\}$$

be the first-hitting time of a δ-neighborhood of the set $\mathcal{M}_q$. Then the expectation of $\tau_{\mathcal{M}_q}$, starting from $u^{(q+1)}$, satisfies

$$\mathbb{E}^{u^{(q+1)}}\{\tau_{\mathcal{M}_q}\} = C(q,n)\,\mathrm{e}^{H_{q+1}/\varepsilon}\big[1 + R_n(\varepsilon)\big]\;,$$

where

$$C(q,n) = \frac{3}{4Kn}\left(1 + \frac{\pi^2(4q+3)-4}{4n}\right) + \mathcal{O}\big(n^{-3}\big)\;, \tag{5.11}$$

$$H_{q+1} = U(u^{(q+1/2)}) - U(u^{(q+1)}) = \frac{K}{\pi} - \left(q + \frac{3}{4}\right)\frac{K\pi}{n} + \mathcal{O}\big(n^{-2}\big)\;, \tag{5.12}$$

$$\lim_{\varepsilon\to 0} R_n(\varepsilon) = 0\;.$$

Proof. The proof is almost an application of [11, Theorem 3.2], which provides an Eyring–Kramers law of the form (2.2), except that we have to deal with degeneracies in the potential landscape. The extra factor n^{-1} in the expected transition time is due to the existence of n saddles, having the same height, each providing an optimal pathway between the q-twisted state $u^{(q+1)}$ and the set $\mathcal{M}_q$. As a result, the integer called k in [11, Equation (3.2)] is equal to n, while the eigenvalues of the saddles are the same for all summands.

The difference between our situation and the one described in [11, Theorem 3.2] is that for any $q \neq 0$, the sinks $u^{(q)}$ and $u^{(-q)}$ are at the same height, as are the relevant saddles. Such symmetric situations have been analysed in [4] for continuous-time Markov chains, and in [16, Chapter 5] for diffusion processes.

In our case, the set of sinks $u^{(q)}$ is invariant under the group $G = \{\mathrm{id}, I\}$, where id is the identity map on the phase space $(\mathbb{R}/\mathbb{Z})^\Lambda$, while I is the inversion given by $I(u) = -u$. Note that G is equivalent to $\mathbb{Z}_2 = \mathbb{Z}/2\mathbb{Z}$. There are two important group-theoretic quantities that influence the Eyring–Kramers law:

- The *orbit* of a point $u \in (\mathbb{R}/\mathbb{Z})^\Lambda$ is defined as the set $O_u = \{g(u)\colon g \in G\}$. In particular, we have $O_{u^{(0)}} = \{u^{(0)}\}$, while $O_{u^{(q)}} = \{u^{(q)}, u^{(-q)}\}$ for $q \neq 0$.
- The *stabiliser* of a point $u \in (\mathbb{R}/\mathbb{Z})^\Lambda$ is defined as the set $G_u = \{g \in G\colon g(u) = u\}$. It is a subgroup of G. In particular, we have $G_{u^{(0)}} = G$, while for $q \neq 0$, $G_{u^{(q)}} = \{\mathrm{id}\}$.

Here, we are concerned with transitions between the orbit $O_{u^{(q+1)}}$, and the union of the orbits from $O_{u^{(0)}}$ to $O_{u^{(q)}}$. For continuous-time Markov chains, [4, Theorem 3.2] states that an Eyring–Kramers law still holds in the symmetric case, but with an extra factor

$$\frac{\#(G_{u^{(q+1)}} \cap G_{u^{(q)}})}{\#(G_{u^{(q+1)}})}\;.$$

However, in our case, we have $\#(G_{u^{(q+1)}} \cap G_{u^{(q)}}) = \#(G_{u^{(q+1)}}) = 1$, so that there is no change to the Eyring–Kramers formula. The same holds true for diffusions, as discussed in [16, Sections 5.2 and 5.3].

The remainder of the proof, providing the asymptotics of the constants, is obtained from (5.1), (5.5), (5.6) and (5.8), along with a Taylor expansion of $\cos(2\pi\hat{q}/n)$ in the large n limit. □

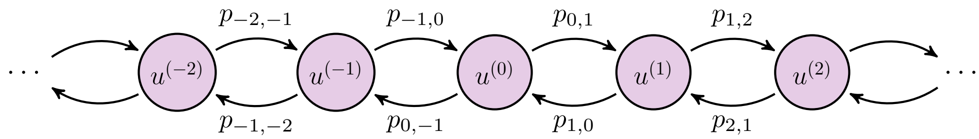

Figure 10: Continuous time Markov chain approximating the dynamics of transitions between q-twisted states.

Remark 5.5.

1. *Figure 14 presents numerical verification of the asymptotics in* (5.11) *and* (5.12)*.*
2. *The above computations would allow us to determine the next-to-leading order of* $C(q,n)$*.*
3. *We do not control how* $R_n(\varepsilon)$ *depends on* n*. In principle, as* n *gets larger, the convergence of* $R_n(\varepsilon)$ *to* 0 *may become slower. However, arguments used in [9] in a somewhat similar situation suggest that this is not the case.*

5.3 More general transitions

In this section, we explain how to compute the expected transition time between more general states, without giving detailed proofs. The basic idea is that the dynamics should be well-approximated by a continuous-time Markov chain on the set of stable q-twisted states, see Figure 10, with transition rates given by

$$p_{q,q+1} = \frac{1}{C_{q,q+1}}\,\mathrm{e}^{-\bar{H}_q/\varepsilon}\;, \qquad p_{q+1,q} = \frac{1}{C_{q+1,q}}\,\mathrm{e}^{-H_q/\varepsilon}$$

for $0 \leqslant q < \frac{n}{4}$, while $p_{-q,-q+1} = p_{q,q+1}$, $p_{-q+1,-q} = p_{q+1,q}$, and $p_{q,\bar{q}} = 0$ if $|\bar{q} - q| \geqslant 2$. Here the coefficients $C_{q,\bar{q}}$ denote the prefactors in the associated Eyring–Kramers laws.

The validity of such a reduction has been analysed in [34, 35] for diffusions, and in [3] for continuous-space Markov chains. To justify this approximation in our situation, we would need to show that the most likely sinks that can be reached from a saddle $u^{(q+1/2)}$ are $u^{(q)}$ and $u^{(q+1)}$, in the sense that the unstable manifolds of the saddle converge to these two sinks. While this is indeed the case for $u^{(q+1)}$, we have not given a full proof of the fact that $u^{(q)}$ is indeed the other sink that the unstable manifold connects to.

Assuming the approximation is indeed justified, expected transition times can be computed as follows. Denote the Markov chain by $(X_t)_{t\geqslant 0}$. It takes values in $\mathcal{X} = \{-m,\dots,m\}$, where $m = \max\{q \in \mathbb{N}_0 \colon q < \frac{n}{4}\}$. Here $q \in \mathcal{X}$ represents the state $u^{(q)}$. Let L denote the infinitesimal generator of the process, that is, the $2m+1$ by $2m+1$ matrix with entries

$$L_{q,\bar{q}} = \begin{cases} p_{q,\bar{q}} & \text{if } \bar{q} \neq q\;, \\ -\sum_{\bar{q}\neq q} p_{q,\bar{q}} & \text{if } \bar{q} = q\;. \end{cases}$$

For a set $A \subset \mathcal{X}$, if

$$w_A(q) = \mathbb{E}^q\{\tau_A\}\;, \qquad \tau_A = \inf\{t > 0 \colon X_t \in A\}\;,$$

we have the relation

$$\sum_{\bar{q}\in A^c} L_{q,\bar{q}} w_A(q) = -1\;. \tag{5.13}$$

For a proof, see for instance [31, Chapter 3].

We give a few examples of applications of (5.13).

1. If $A^c = \{0\}$, then τ_A denotes the first-hitting time of any sink different from $u^{(0)}$. In that case, we obtain
$$\mathbb{E}^0\{\tau_A\} = \frac{1}{p_{0,1} + p_{0,-1}} = \frac{1}{2p_{0,1}} = \frac{1}{2} C_{01}\, \mathrm{e}^{\bar{H}_0/\varepsilon} .$$
Here the factor $\frac{1}{2}$ is due to the fact that there is an equal probability to escape towards positive and negative q.

2. If $A^c = \{q\}$ for some $q \neq 0$, say $q > 0$, then τ_A denotes again the first-hitting time of any sink different from $u^{(q)}$. Then we find
$$\mathbb{E}^q\{\tau_A\} = \frac{1}{p_{q,q+1} + p_{q,q-1}} = \frac{C_{q,q-1}\, \mathrm{e}^{H_q/\varepsilon}}{1 + \frac{C_{q,q-1}}{C_{q,q+1}}\, \mathrm{e}^{-[\bar{H}_q - H_q]/\varepsilon}} .$$
It follows from Lemma 5.1 that
$$\bar{H}_q - H_q = \frac{K\pi}{2n} + \mathcal{O}\big(n^{-2}\big) .$$
Therefore, for finite n, the expectation is dominated by transitions to $u^{(q-1)}$, and hence $\mathbb{E}^q\{\tau_A\} \simeq C_{q,q-1}\, \mathrm{e}^{H_q/\varepsilon}$.

3. As a more complicated example, let us look at the case where $A^c = \{-1, 0, 1\}$. Then we have to solve the system
$$\begin{pmatrix} -(L_{-1,-2} + L_{-1,0}) & L_{-1,0} & 0 \\ L_{0,-1} & -(L_{0,-1} + L_{0,1}) & L_{0,1} \\ 0 & L_{1,0} & -(L_{1,0} + L_{1,2}) \end{pmatrix} \begin{pmatrix} w_A(-1) \\ w_A(0) \\ w_A(1) \end{pmatrix} = \begin{pmatrix} -1 \\ -1 \\ -1 \end{pmatrix} .$$
The symmetry $L_{q,\bar{q}} = L_{-q,-\bar{q}}$ implies $w_A(-1) = w_A(1)$. This yields an effective two-dimensional system, whose solution is
$$\mathbb{E}^0\{\tau_A\} = w_A(0) = \frac{2L_{0,1} + L_{1,0} + L_{1,2}}{2L_{0,1}L_{1,2}} ,$$
$$\mathbb{E}^1\{\tau_A\} = w_A(1) = \frac{2L_{0,1} + L_{1,0}}{2L_{0,1}L_{1,2}} .$$
For finite n, we have $\bar{H}_1 > \bar{H}_0 > H_1$, which implies $L_{1,2} \ll L_{0,1} \ll L_{1,0}$. This implies that there exists a constant $\theta > 0$, of order n^{-1}, such that
$$\mathbb{E}^0\{\tau_A\} = \frac{C_{0,1}C_{1,2}}{2C_{1,0}}\, \mathrm{e}^{[\bar{H}_0 - H_1 + \bar{H}_2]/\varepsilon}\big[1 + \mathcal{O}(\mathrm{e}^{-\theta/\varepsilon})\big] ,$$
$$\mathbb{E}^1\{\tau_A\} = \frac{C_{0,1}C_{1,2}}{2C_{1,0}}\, \mathrm{e}^{[\bar{H}_0 - H_1 + \bar{H}_2]/\varepsilon}\big[1 + \mathcal{O}(\mathrm{e}^{-\theta/\varepsilon})\big] .$$
In other terms, the expected first-hitting time does not depend on the starting point to leading order. What happens is that if the system starts in state $u^{(1)}$, it will, with overwhelming probability, visit state $u^{(0)}$ before any other state. Note that the exponent $\bar{H}_0 - H_1 + \bar{H}_2$ is equal to the potential difference $V(u^{(3/2)}) - V(u^{(0)})$, which is precisely the relative communication height between the states $u^{(0)}$ and $u^{(2)}$.

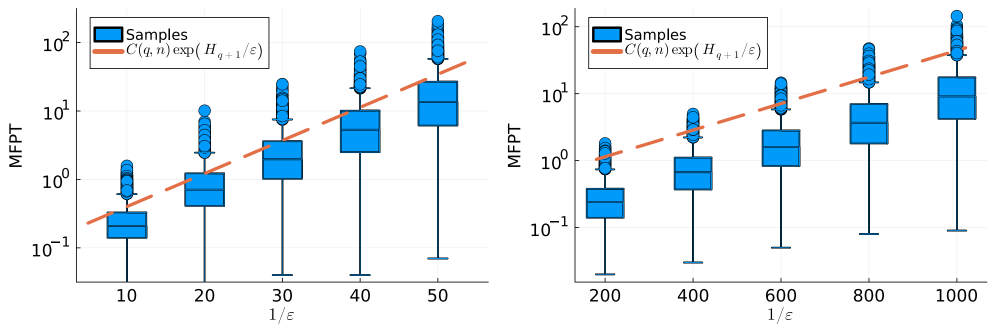

(a) $q = 0$ (b) $q = 1$

Figure 11: Empirical first passage time distributions for the $n = 10$ system, compared against the Eyring–Kramers formula (2.2). For each value of ε, 10^4 independent trials were performed.

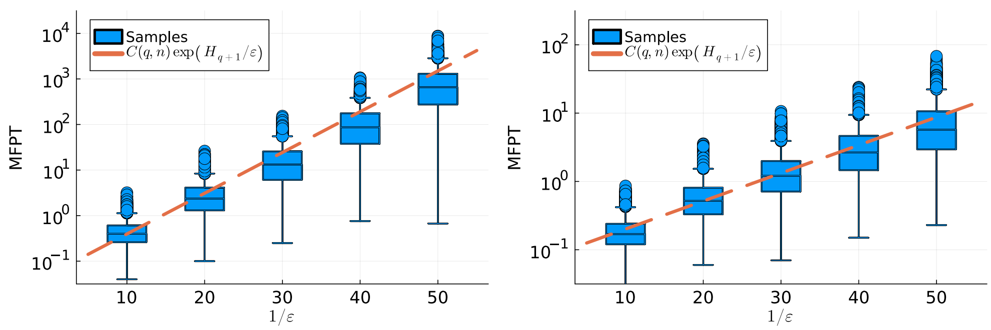

(a) $q = 0$ (b) $q = 1$

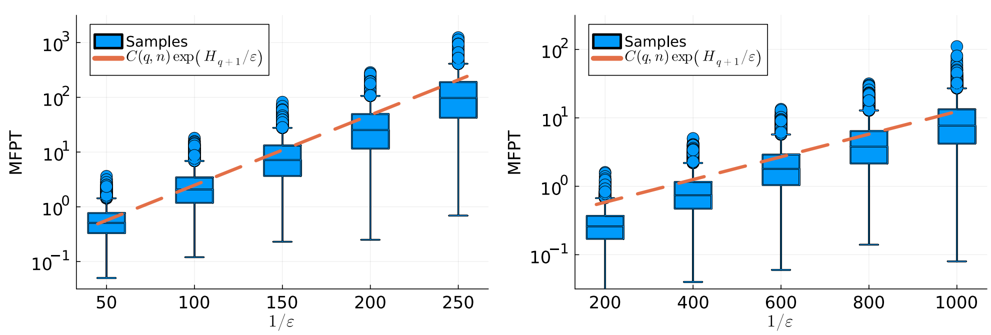

(c) $q = 2$ (d) $q = 3$

Figure 12: Empirical first passage time distributions for the $n = 20$ system, compared against the Eyring–Kramers formula (2.2). For each value of ε, 10^4 independent trials were performed.

6 Numerical simulations

In this section, we provide numerical simulations illustrating our main results, as well as some extensions to more general couplings.

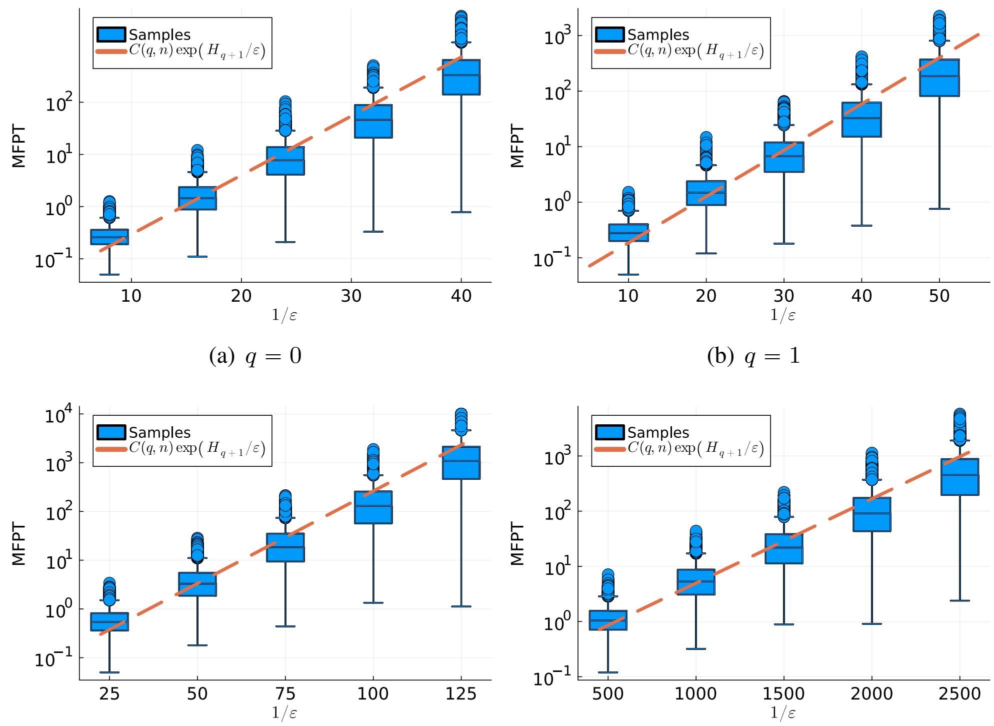

(a) $q = 0$ (b) $q = 1$ (c) $q = 3$ (d) $q = 7$

Figure 13: Empirical first passage time distributions for the $n = 40$ system, compared against the Eyring–Kramers formula (2.2). For each value of ε, 10^4 independent trials were performed.

6.1 Eyring–Kramers asymptotics for the Kuramoto model

Our first numerical result verifies the Eyring–Kramers law (2.2) for the Kuramoto problem. This is done directly by running independent trials of (1.2), with initial conditions given by one of the twisted states. As shown in Figures 11, 12, and 13, we have good agreement between the data and the law. Though some cases have closer agreement of the sample means than others, the trends are consistent across all cases and the error is well under an order of magnitude.

We note that we are comparing against the *exact* Eyring–Kramers formula, and not the asymptotic expansion obtained in Theorem 5.4. In each problem, 10^4 independent trials were performed with $\Delta t = 10^{-2}$ using Euler–Maruyama time stepping (see [27] for additional details). Detection of an escape from the basin of attraction was performed by using a BFGS routine (see [22, 30]) to minimize the energy U at the current state of the system. Values of ε were chosen for each problem such that we had

$$1 \lesssim H_{q+1}/\varepsilon \lesssim 10.$$

This makes the problems sufficiently low temperature such that the system is entering the Arrhenius regime, but not so low as to require advanced rare event simulation techniques.

6.2 Sharp asymptotics of the prefactor and the energy barrier

Next, we confirm the predictions of Theorem 5.4 by numerically computing the prefactor $C(q, n)$ and energy barrier H_{q+1}, then comparing them against the asymptotic formulae. As shown in Figure 14, subject to a rescaling, we have the anticipated behavior for $q = 0, 1, 2, 3$ across a broad

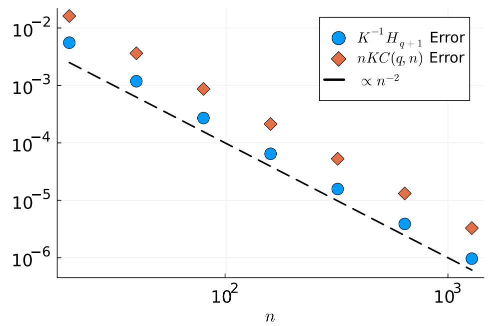

(a) $q = 0$

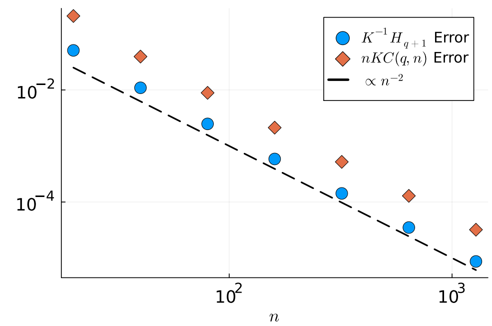

(b) $q = 1$

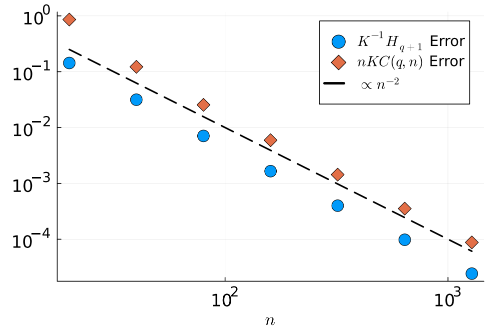

(c) $q = 2$

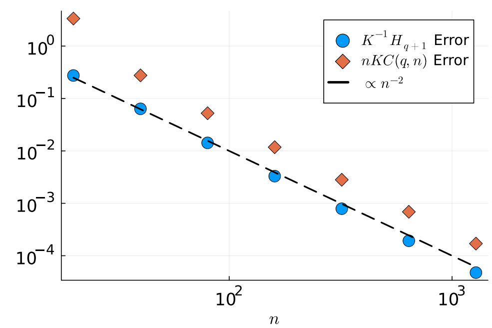

(d) $q = 3$

Figure 14: Confirmation that, after rescaling, the constants $C(q, n)$ and H_{q+1} obey the predictions of (5.11) and (5.12) in the large n limit.

range of n. These were computed by direct evaluation of the energy and the eigenvalues of the Hessian for the relevant states.

6.3 Beyond nearest neighbor interaction

Thus far, our study has been focused on the case of nearest neighbor interactions ($r = 1$), but part of what makes Kuramoto models so interesting is their behavior when longer range interactions are included [13,26,29,33,38]. While we do not pursue a full numerical or analytic study here, we conclude with some computations of the energy barriers and prefactors. These were computed by finding the saddle point states using the string method and the climbing image method (cf. [17]).

We consider the case of the system with $r > 1$ nearest neighbors, and varying the system size, n, for several values of q. As shown in Figure 15, we see the following properties. First, as is consistent with (5.11) for the $r = 1$ case, as $n \to \infty$, $nC(q, n)$ tends to a finite positive constant, independent of q. Additionally, larger q values, at fixed n, have larger prefactors. Analogous to (5.12), energy barrier H_{q+1} tends to a a fixed constant. At fixed n, larger values of q have lower energy barriers. We thus conjecture that formulas analogous to (5.11) and (5.12) are also valid in the nonlocal case.

7 Discussion

In this work, we have described metastable transitions in a Kuramoto model with nearest-neighbor interaction, for arbitrary but finite number n of oscillators. In particular, we have shown that the

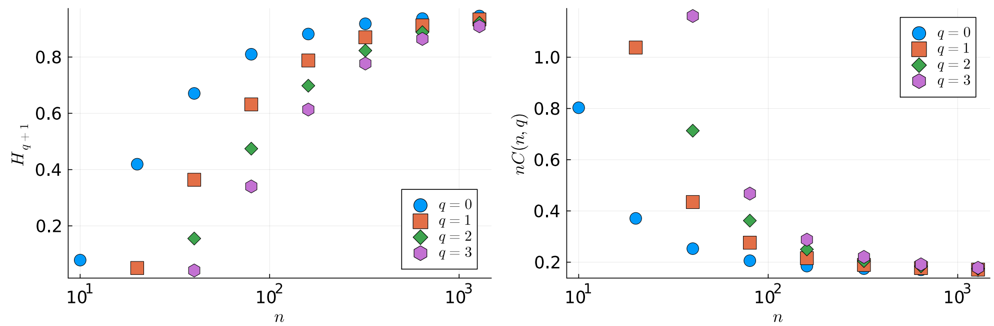

(a) $r = 2$ (b) $r = 2$

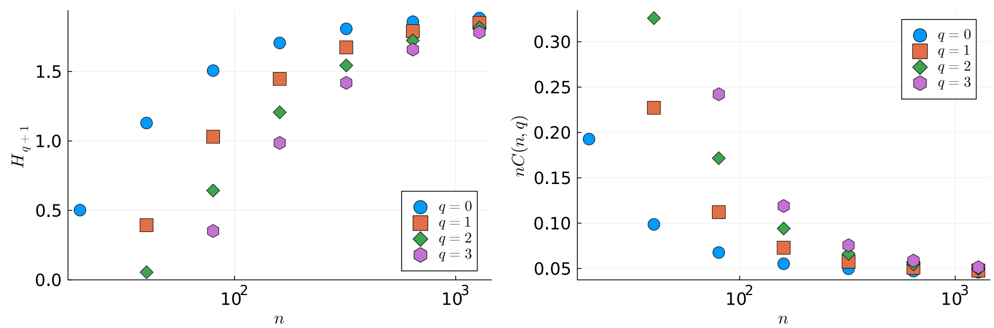

(c) $r = 3$ (d) $r = 3$

Figure 15: Energy barriers and prefactors for the Eyring–Kramers formula in the case of $r > 1$ nearest neighbors for several twisted states.

most likely transitions are those between q-twisted states $u^{(q_1)}$ and $u^{(q_2)}$ with $|q_2| < |q_1|$, and obtained sharp Eyring–Kramers-type asymptotics for the expected transition time.

One interesting question is, what happens in the limit $n \to \infty$. Consider a sequence of systems on $\Lambda_n = \mathbb{Z}/n\mathbb{Z}$, given by

$$\mathrm{d}u_i = K_n\big[\sin\big(2\pi(u_{i+1} - u_i)\big) + \sin\big(2\pi(u_{i-1} - u_i)\big)\big]\,\mathrm{d}t + \sqrt{2\varepsilon_n}\,\mathrm{d}W_t^i \;.$$

Assume that there exists a smooth interpolating function $\phi(t, x)$, such that

$$u_i = \phi\left(t, \frac{i}{n}\right) \qquad \forall i \in \Lambda_n \;.$$

Since

$$\sin\big(2\pi(u_{i\pm1} - u_i)\big) = \pm\frac{2\pi}{n}\partial_x\phi\left(t, \frac{i}{n} \pm \frac{1}{2n}\right) + \mathcal{O}\left(\frac{1}{n^3}\right) ,$$

we obtain that ϕ satisfies the equation

$$\mathrm{d}\phi(t,x) = \left[\frac{2\pi K_n}{n^2}\partial_{xx}\phi(t,x) + \mathcal{O}\left(\frac{1}{n^3}\right)\right]\mathrm{d}t + \sqrt{2\varepsilon_n}\,\mathrm{d}W(t,x) \;, \tag{7.1}$$

where $\mathrm{d}W(t,x)$ denotes space-time white noise. One natural scaling regime is obtained by setting $K_n = n^2$. If we choose $\varepsilon_n = \varepsilon$ to be constant, (7.1) converges formally to a stochastic heat equation on the torus, where ϕ also has values in the torus.

Note however that the relative communication height between q-twisted states satisfies

$$H_n = \frac{K_n}{\pi}\biggl(1 + \mathcal{O}\biggl(\frac{1}{n}\biggr)\biggr) .$$

Therefore, to leading order, the mean transition time between q-twisted states is given by

$$\frac{3\pi}{2n}\,\mathrm{e}^{K_n/(\pi\varepsilon_n)} .$$

This time diverges as $n \to \infty$ if $K_n = n^2$ and $\varepsilon_n = \varepsilon$ (this is of course assuming that the error term $R_n(\varepsilon)$ in Theorem 5.4 remains bounded, which we have not proved). The interpretation of this is that because of the jump discontinuity of the 1-saddles u^r, r a half-integer, these states do not converge to continuous functions in the continuum limit. Instead, they have an infinite slope at one point, and this makes their energy blow up. As a result, we do not expect to see any metastable transitions in the continuum limit, at least for this particular scaling.

This may change, however, when one goes beyond nearest-neighbor coupling. Assume that the coupling set S in (1.1) is given by

$$S = \bigl\{-r(n), \dots, r(n)\bigr\}$$

so that the range is $r(n)$. As discussed in Section 6.3, numerical simulations indicate that similar Eyring–Kramers asymptotics as those obtained for nearest-neighbor coupling hold for general interaction ranges. If $r(n)$ scales like a constant times n, 1-saddles visited during transitions between q-twisted states may have a smoother space dependence, in which the jump is replaced by a boundary layer. For suitable parameter values, this could imply that these transition states have a finite energy in the $n \to \infty$ limit, which would result in a finite value for the expectation of metastable transition times.

Acknowledgement

NB was supported by the ANR project PERISTOCH, ANR–19–CE40–0023. The work of GM was partially supported by National Science Foundation (NSF) through grants DMS–2009233 and DMS–2406941. GS was supported by NSF grant number DMS–2111278. Work reported here was run on hardware supported by Drexel's University Research Computing Facility.

This work was motivated by numerical experiments conducted by a group of undergraduate students during two NSF supported summer REUs at Drexel University. John Bonnes, Nicholas De Filippis, Zachary Lee, and Jacob Woods contributed at the early stages of this project.

References

[1] D.M. Abrams and S.H. Strogatz, *Chimera states in a ring of nonlocally coupled oscillators*, Internat. J. Bifur. Chaos Appl. Sci. Engrg. **16** (2006), no. 1, 21–37. MR 2214910 (2006k:37043)

[2] Nils Berglund, *Kramers' law: validity, derivations and generalisations*, Markov Process. Related Fields **19** (2013), no. 3, 459–490. MR 3156961

[3] ———, *Reducing metastable continuous-space Markov chains to Markov chains on a finite set*, `arXiv/2303.12624`, to appear in Annales de l'Institut Henri Poincaré (2023).

[4] Nils Berglund and Sébastien Dutercq, *The Eyring-Kramers law for Markovian jump processes with symmetries*, J. Theoret. Probab. **29** (2016), no. 4, 1240–1279. MR 3571245

[5] ———, *Interface Dynamics of a Metastable Mass-Conserving Spatially Extended Diffusion*, J. Stat. Phys. **162** (2016), no. 2, 334–370. MR 3441363

[6] Nils Berglund, Bastien Fernandez, and Barbara Gentz, *Metastability in interacting nonlinear stochastic differential equations. I. From weak coupling to synchronization*, Nonlinearity **20** (2007), no. 11, 2551–2581. MR 2361246

[7] ———, *Metastability in interacting nonlinear stochastic differential equations. II. Large-N behaviour*, Nonlinearity **20** (2007), no. 11, 2583–2614. MR 2361247

[8] Nils Berglund and Barbara Gentz, *The Eyring–Kramers law for potentials with nonquadratic saddles*, Markov Processes Relat. Fields **16** (2010), 549–598. MR 2759772 (2011i:60139)

[9] ———, *Sharp estimates for metastable lifetimes in parabolic SPDEs: Kramers' law and beyond*, Electron. J. Probab. **18** (2013), no. 24, 1–58.

[10] Anton Bovier and Frank den Hollander, *Metastability. A potential-theoretic approach*, Grundlehren Math. Wiss., vol. 351, Cham: Springer, 2015 (English).

[11] Anton Bovier, Michael Eckhoff, Véronique Gayrard, and Markus Klein, *Metastability in reversible diffusion processes. I: Sharp asymptotics for capacities and exit times*, J. Eur. Math. Soc. (JEMS) **6** (2004), no. 4, 399–424 (English).

[12] Hayato Chiba and Georgi S. Medvedev, *The mean field analysis of the Kuramoto model on graphs I. The mean field equation and transition point formulas*, Discrete Contin. Dyn. Syst. **39** (2019), no. 1, 131–155. MR 3918168

[13] Hayato Chiba, Georgi S. Medvedev, and Matthew S. Mizuhara, *Bifurcations in the Kuramoto model on graphs*, Chaos **28** (2018), no. 7, 073109, 10.

[14] Lee DeVille, *Transitions amongst synchronous solutions in the stochastic Kuramoto model*, Nonlinearity **25** (2012), no. 5, 1473–1494. MR 2914150

[15] Florian Dörfler and Francesco Bullo, *Synchronization in complex networks of phase oscillators: a survey*, Automatica J. IFAC **50** (2014), no. 6, 1539–1564. MR 3214901

[16] Sébastien Dutercq, *Métastabilité dans les systèmes avec lois de conservation*, Ph.D. thesis, University of Orléans, 2015.

[17] Weinan E, Weiqing Ren, and Eric Vanden-Eijnden, *Simplified and improved string method for computing the minimum energy paths in barrier-crossing events*, Journal of Chemical Physics **126** (2007), no. 16, 164103.

[18] M. I. Freidlin, *Sublimit distributions and the stabilization of the solutions of parabolic equations with a small parameter*, Dokl. Akad. Nauk SSSR **235** (1977), no. 5, 1042–1045. MR 454349

[19] Mark I. Freidlin and Alexander D. Wentzell, *Random perturbations of dynamical systems*, third ed., Grundlehren der mathematischen Wissenschaften [Fundamental Principles of Mathematical Sciences], vol. 260, Springer, Heidelberg, 2012, Translated from the 1979 Russian original by Joseph Szücs. MR 2953753

[20] Giambattista Giacomin, Eric Luçon, and Christophe Poquet, *Coherence stability and effect of random natural frequencies in populations of coupled oscillators*, J. Dyn. Differ. Equations **26** (2014), no. 2, 333–367 (English).

[21] Giambattista Giacomin, Christophe Poquet, and Assaf Shapira, *Small noise and long time phase diffusion in stochastic limit cycle oscillators*, J. Differ. Equations **264** (2018), no. 2, 1019–1049 (English).

[22] Michael T. Heath, *Scientific computing: an introductory survey*, revised second edition, siam edition ed., Classics in applied mathematics, no. 80, Society for Industrial and Applied Mathematics, Philadelphia, 2018 (en).

[23] Y. Kuramoto and D. Battogtokh, *Coexistence of coherence and incoherence in nonlocally coupled phase oscillators*, Nonlinear Phenomena in Complex Systems **5** (2002), 380–385.

[24] Yoshiki Kuramoto, *Self-entrainment of a population of coupled non-linear oscillators*, International Symposium on Mathematical Problems in Theoretical Physics (Kyoto Univ., Kyoto, 1975), Springer, Berlin, 1975, pp. 420–422. Lecture Notes in Phys., 39. MR 0676492

[25] E. Luçon and C. Poquet, *Long time dynamics and disorder-induced traveling waves in the stochastic Kuramoto model*, Ann. Inst. Henri Poincaré, Probab. Stat. **53** (2017), no. 3, 1196–1240 (English).

[26] Georgi S. Medvedev and Matthew S. Mizuhara, *Chimeras unfolded*, J. Stat. Phys. **186** (2022), no. 3 (English).

[27] Georgi S. Medvedev and Gideon Simpson, *A numerical method for a nonlocal diffusion equation with additive noise*, Stochastics and Partial Differential Equations: Analysis and Computations **11** (2023), 1433–1469.

[28] Georgi S. Medvedev and Svitlana Zhuravytska, *The geometry of spontaneous spiking in neuronal networks*, J. Nonlinear Sci. **22** (2012), no. 5, 689–725. MR 2982050

[29] G.S. Medvedev and X. Tang, *Stability of twisted states in the Kuramoto model on Cayley and random graphs*, Journal of Nonlinear Science **25** (2015), 1169–1208.

[30] Jorge Nocedal and Stephen J. Wright, *Numerical optimization*, 2nd ed ed., Springer series in operations research, Springer, New York, 2006 (en), OCLC: ocm68629100.

[31] J.R. Norris, *Markov chains*, Cambridge University Press, 2006.

[32] Enzo Olivieri and Maria Eulália Vares, *Large deviations and metastability*, Encyclopedia of Mathematics and its Applications, vol. 100, Cambridge University Press, Cambridge, 2005. MR 2123364

[33] O. E. Omel'chenko, *The mathematics behind chimera states*, Nonlinearity **31** (2018), no. 5, R121–R164. MR 3816650

[34] Fraydoun Rezakhanlou and Insuk Seo, *Scaling limit of small random perturbation of dynamical systems*, Preprint `arXiv/1812.02069`, 2018.

[35] Insuk Seo, *Analysis of metastable behavior via solutions of Poisson equations*, RIMS Kôkyûroku Bessatsu **B79** (2020), 1–17 (English).

[36] Steven H. Strogatz, *From Kuramoto to Crawford: exploring the onset of synchronization in populations of coupled oscillators*, **143**, no. 1, 1–20.

[37] ———, *Sync*, Hyperion Books, New York, 2003, How order emerges from chaos in the universe, nature, and daily life. MR 2394754

[38] D.A. Wiley, S.H. Strogatz, and M. Girvan, *The size of the sync basin*, Chaos **16** (2006), no. 1, 015103, 8. MR 2220552 (2007e:37016)

Nils Berglund
Institut Denis Poisson (IDP)
Université d'Orléans, Université de Tours, CNRS – UMR 7013
Bâtiment de Mathématiques, B.P. 6759
45067 Orléans Cedex 2, France
E-mail address: `nils.berglund@univ-orleans.fr`

Georgi S. Medvedev
Department of Mathematics
Drexel University
3141 Chestnut Street
Philadelphia, PA 19104, USA
E-mail address: `medvedev@drexel.edu`

Gideon Simpson
Department of Mathematics
Drexel University
3141 Chestnut Street
Philadelphia, PA 19104, USA
E-mail address: `grs53@drexel.edu`